Table 1. continued

gene ID	symbol	description	refs
3932	LCK	lymphocyte-specific protein tyrosine kinase	22
55679	LIMS2	LIM and senescent cell antigen-like domains 2	22
4067	LYN	v-yes-1 Yamaguchi sarcoma viral related oncogene homologue	22
9448	MAP4K4	mitogen-activated protein kinase kinase kinase kinase 4	this study
6300	MAPK12	mitogen-activated protein kinase 12	22
4155	MBP	myelin basic protein	22
4256	MGP	matrix Gla protein	110
55233	MOB1A	MOB kinase activator 1A	22
4673	NAP1L1	nucleosome assembly protein 1-like 1	22
4674	NAP1L2	nucleosome assembly protein 1-like 2	22
10397	NDRG1	N-myc downstream regulated 1	22
4778	NFE2	nuclear factor (erythroid-derived 2), 45 kDa	22
11188	NISCH	nischarin	this study
4924	NUCB1	nucleobindin 1	22
4938	OAS1	2′-5′-oligoadenylate synthetase 1, 40/46 kDa	22
5007	OSBP	oxysterol binding protein	111
64098	PARVG	parvin, gamma	22
5170	PDPK1	3-phosphoinositide dependent protein kinase-1	22
5297	PI4KA	phosphatidylinositol 4-kinase, catalytic, alpha	22
5291	PIK3CB	phosphoinositide-3-kinase, catalytic, beta polypeptide	22
5295	PIK3R1	phosphoinositide-3-kinase, regulatory subunit 1 (alpha)	55,84,106
5300	PIN1	peptidylprolyl cis/trans isomerase, NIMA-interacting 1	112
5307	PITX1	paired-like homeodomain 1	22
5347	PLK1	polo-like kinase 1	113
10654	PMVK	phosphomevalonate kinase	22
5478	PPIA	peptidylprolyl isomerase A (cyclophilin A)	114,115
10848	PPP1R13L	protein phosphatase 1, regulatory subunit 13 like	22
5515	PPP2CA	protein phosphatase 2, catalytic subunit, alpha isozyme	116
5518	PPP2R1A	protein phosphatase 2, regulatory subunit A, alpha	116
5698	PSMB9	proteasome (prosome, macropain) subunit, beta type, 9 (large multifunctional peptidase 2)	22
5757	PTMA	prothymosin, alpha	22
5894	RAF1	v-raf-1 murine leukemia viral oncogene homologue 1	22
6142	RPL18A	ribosomal protein L18a	22
6167	RPL37	ribosomal protein L37	this study
6238	RRBP1	ribosome binding protein 1 homologue 180 kDa (dog)	22
91543	RSAD2	radical S-adenosyl methionine domain containing 2	117
6252	RTN1	reticulon 1	this study
10313	RTN3	reticulon 3	this study
6424	SFRP4	secreted frizzled-related protein 4	22
81858	SHARPIN	SHANK-associated RH domain interactor	22
64754	SMYD3	SET and MYND domain containing 3	22
8470	SORBS2	sorbin and SH3 domain containing 2	22
10174	SORBS3	sorbin and SH3 domain containing 3	22
6714	SRC	v-src sarcoma (Schmidt-Ruppin A-2) viral oncogene homologue (avian)	22
10847	SRCAP	Snf2-related CREBBP activator protein	22
6741	SSB	Sjogren syndrome antigen B (autoantigen La)	22
284297	SSC5D	scavenger receptor cysteine rich domain containing (5 domains)	110
6772	STAT1	signal transducer and activator of transcription 1	118
25777	SUN2	Sad1 and UNC84 domain containing 2	this study
6850	SYK	spleen tyrosine kinase	119
4070	TACSTD2	tumor-associated calcium signal transducer 2	22
6880	TAF9	TAF9 RNA polymerase II, TATA box binding protein (TBP)-associated factor, 32 kDa	22
6908	TBP	TATA box binding protein	22
7046	TGFBR1	transforming growth factor, beta receptor 1	22
7057	THBS1	thrombospondin 1	22
374395	TMEM179B	transmembrane protein 179B	22
7110	TMF1	TATA element modulatory factor 1	22
7157	TP53	tumor protein p53	22
7159	TP53BP2	tumor protein p53 binding protein, 2	22
7186	TRAF2	TNF receptor-associated factor 2	22
11078	TRIOBP	TRIO and F-actin binding protein	22

Table 1. continued

gene ID	symbol	description	refs
51061	TXNDC11	thioredoxin domain containing 11	22
53347	UBASH3A	ubiquitin associated and SH3 domain containing A	22
10869	USP19	ubiquitin specific peptidase 19	22
9218	VAPA	VAMP (vesicle-associated membrane protein)-associated protein A, 33 kDa	22
9217	VAPB	VAMP (vesicle-associated membrane protein)-associated protein B and C	this study; 22,28,46
10493	VAT1	vesicle amine transport protein 1 homologue (*T. californica*)	this study
55737	VPS35	vacuolar protein sorting 35 homologue (*S. cerevisiae*)	22
6293	VPS52	vacuolar protein sorting 52 homologue (*S. cerevisiae*)	22
140612	ZFP28	zinc finger protein 28 homologue (mouse)	this study
9726	ZNF646	zinc finger protein 646	22

Quantitative Reverse-Transcription PCR (qRT-PCR)

Total RNA was prepared from the cell and culture supernatant using the RNeasy mini kit (QIAGEN, Hilden, Germany) and QIAamp Viral RNA Mini Kit (QIAGEN), respectively. First-strand cDNA was synthesized using high capacity cDNA reverse transcription kit (Applied biosystems, Carlsbad, CA, USA) with random primers. Each cDNA was estimated by Platinum SYBR Green qPCR Super Mix UDG (Invitrogen) as per the manufacturer's protocol. Fluorescent signals of SYBR Green were analyzed with ABI PRISM 7000 (Applied Biosystems). The HCV internal ribosomal entry site (IRES) region and human glyceraldehyde-3-phosphate dehydrogenase (GAPDH) gene were amplified with the primer pairs 5′-GAGTGTCGTGCAGCCTCCA-3′ and 5′-CACTCG-CAAGCACCCTATCA-3′, and 5′-GAAGGTCGGAGT-CAACGGATT-3′ and 5′-GATGACAAGCTTCCCGTTCTC-3′, respectively.[42] The quantities of the HCV genome and the other host mRNAs were normalized with that of GAPDH mRNA. RTN1 and RTN3 genes were amplified using the primer pairs purchased from QIAGEN.

Cell Lines and Virus Infection

Cells from the Huh7OK1 cell line are highly permissive to HCV JFH1 strain (genotype 2a) infection compared to Huh 7.5.1 and exhibit the highest propagation efficiency for JFH1.[43] These cells were maintained at 37 °C in a humidified atmosphere and 5% CO_2, in the Dulbecco's modified Eagle's medium (DMEM) (Sigma, St. Louis, MO, USA) supplemented with nonessential amino acids (NEAA) and 10% fetal calf serum (FCS). The viral RNA of JFH1 was introduced into Huh7OK1 as described by Wakita et al.[44] The viral RNA of JFH1 derived from the plasmid pJFH1 was prepared as described by Wakita et al.[44]

Statistical Analysis

Experiments for RNAi transfection and qRT-PCR were performed two times. The estimated values were represented as the mean ± standard deviation (n = 2). The significance of differences in the means was determined by the Student's t-test.

RESULTS AND DISCUSSION

Identifying Host Proteins That Interact with HCV NS5A Protein

We employed an integrated approach that combined an experimental Y2H assay and comprehensive literature mining to identify human host proteins interacting with NS5A.

First, we performed an Y2H screening to characterize the interactions between NS5A and host proteins. The analysis of positive colonies revealed 17 host factors as interacting partners of NS5A (Tables 1, S1, Supporting Information), 14 of which are novel. The other three interactions have been characterized previously; vesicle-associated membrane protein (VAMP)-associated protein B (VAPB), a membrane trafficking factor, and FK506-binding protein 8 (FKBP8), an immunoregulation protein, independently regulate HCV replication via interactions with NS5A;[28,43,45,46] Bridging integrator 1 (BIN1), a tumor suppressor protein, interacts with NS5A and significantly contributes to HCC.[47] Among the newly discovered interactors, MAP4K4 is overexpressed in HCC, and knockdown of MAP4K4 expression inhibits HCC progression;[48] RTN1 and VAT1 were previously observed to be elevated in HCV infected cells,[49] and ARL6IP1, EPHB6, GABARAPL2, ITSN1 and NISCH were differentially expressed in HCV infection in vitro.[50] Furthermore, five (ARL6IP1, FKBP8, RTN1, RTN3, VAPB) of the 17 interactors (29.4%) localize to the endoplasmic reticulum (ER; GO:0005783; p = 0.0028), which is consistent with the role of NS5A as a crucial constituent of the HCV replication complex associated with the ER.[51] These results suggest that the PPIs detected by our Y2H assay may closely reflect NS5A interactions in vivo.

We next scanned the biomedical literature to expand the repertoire of NS5A–host interactions. Because of an ever increasing volume of biomedical literature describing the pathogenesis of infectious diseases, the identification of specific host–pathogen interactions and their roles in pathogenicity is a nontrivial task, and therefore, recent years have witnessed a rapid development of computational tools for biomedical literature mining. We performed extensive literature mining using computational tools that facilitate the retrieval and extraction of relevant information from the biomedical literature (Pubmed, EBIMed, Protein Coral) and followed it up with a careful manual inspection to identify additional host factors, which directly interact with NS5A and which were not present in the Y2H data set. One hundred and fifteen pairwise interactions between NS5A and human proteins (consisting of 93 catalogued by a high throughput study of binary HCV–host interactions[22] and 22 from assorted reports; see Supporting Information, Table S2) were extracted from the literature in this manner and were added to the existing interactors. The resulting NS5A–human interactome thus comprised 132 human host proteins directly interacting with NS5A (Table 1), all of which are expressed in the liver (see Supporting Information, Table S3).

Network Topological Analysis of the NS5A–host Interactions: NS5A Preferentially Targets Hubs and Bottlenecks in the Host Protein Interactome

To further understand the biological significance of the NS5A–host interactions, we retrieved PPIs for the nodes targeted by

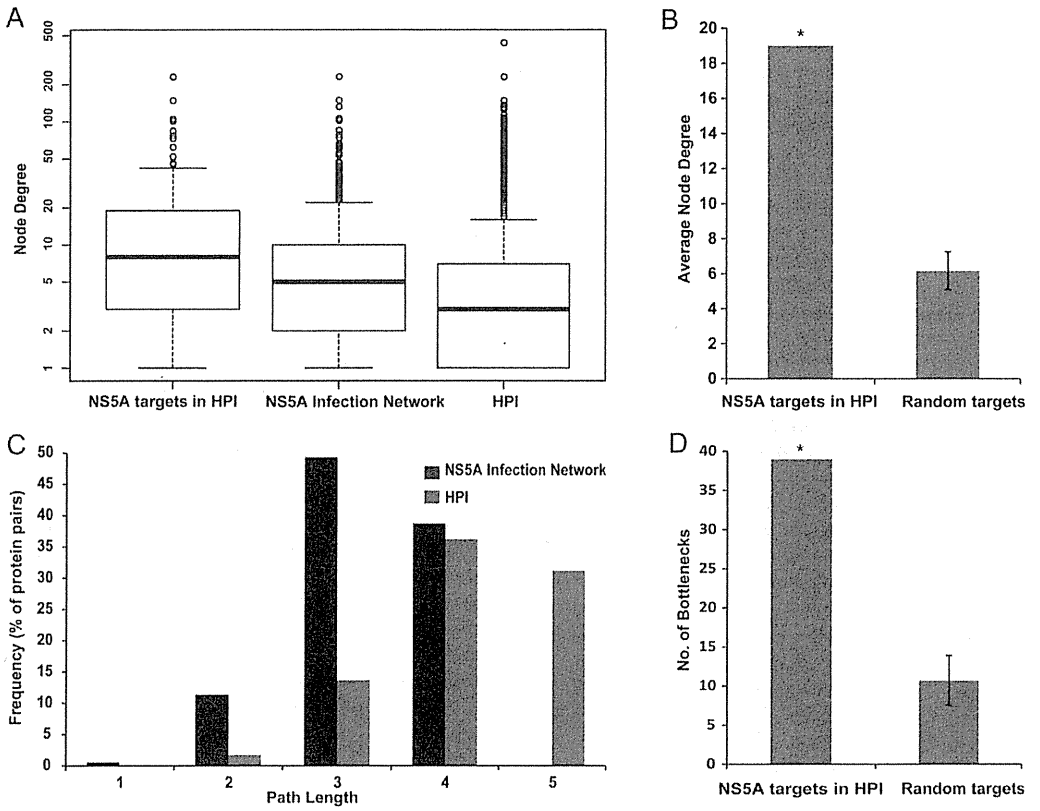

Figure 1. Topological analysis of the NS5A infection network. (A) The node degree distributions of the NS5A interatcors in the HPI, NS5A infection network, and HPI are represented as box plots. The average degree of the NS5A interactors in HPI (19.02) was higher than those of the NS5A infection network (8.24) and HPI (5.96). Median node degrees (indicated by thick horizontal lines) of the NS5A interactors in HPI, NS5A infection network, and HPI are 8, 5, and 3, respectively. (B) The average degree of the nodes targeted by NS5A in HPI was much higher than mean average degree of 1000 sets of the randomly selected 108 nodes in HPI. (C) The shortest path length distributions of the NS5A infection network and HPI. The path length is represented on the *x*-axis while the *y*-axis describes the frequency, i.e., the percentage of node (protein) pairs within the PPI network with a given shortest path length. For simplicity, only the node frequencies for path lengths 1−5 in the HPI are displayed. (D) The number of bottlenecks among the nodes targeted by NS5A in HPI was much higher than mean of the number of bottlenecks among 1000 sets of the randomly selected 108 nodes in HPI. *: $p < 0.001$.

NS5A in the HPI and incorporated them with the initial interactions to infer an extended NS5A infection network. PPIs for 108 of 132 NS5A interactors were retrieved in this manner; 24 of 132 NS5A interactors had no PPIs in the HPI (Supporting Information, Tables S4, S5a, S5b). For the NS5A infection network and the HPI, we computed the node degree distribution and the characteristic/average path length measures to capture the topologies of the two networks. The degree of a protein, which corresponds to the number of its interacting partners, may often reflect its biological relevance since a better connected protein is likely to have a higher ability to influence biological networks via PPIs. Average path lengths provide an approximate measure of the relative ease and speed of dissemination of information between the proteins in a network.

The NS5A infection network consisted of 1442 entities (nearly all of which are expressed in the liver; see Supporting Information) with 6263 interactions between them (Supporting Information, Tables S4, S5a). The average degree (defined as the number of interactions for a given protein) of the NS5A infection network (8.24) was notably higher than the degree inferred for the HPI (5.96) (Figure 1A). Furthermore, the average degree of the nodes targeted by NS5A in the HPI (19.02) was even higher; this number is significantly greater than the average degree obtained from a sample of randomly selected nodes (6.17 ± 1.08 with $p < 0.001$; Figure 1B; see Supporting Information). Also the degrees inferred for the majority of the NS5A interactors in the HPI (65 of 108; 60.18%) were higher than the mean degree of the HPI (5.96) (Figure 1A). Our observations therefore suggest that NS5A preferentially targets several highly connected cellular proteins (hubs) with an ability to influence a large number of host factors in HCV infection. The average (shortest) path length of the NS5A infection network (3.26) was significantly shorter than the HPI (4.54), and also the distribution of shortest path lengths was shifted toward the left (Figure 1C), thereby suggesting that the NS5A influenced cellular network is more compact and inclined toward faster communication between the constituents relative to the host cellular network.

Next, we examined the betweenness measures of the NS5A interactors in the HPI to assess their significance in the HPI and the NS5A infection network. The betweenness of a node, determined by the number of shortest paths passing through it, reflects the importance of that node in the network; the nodes

with the highest betweenness prominently regulate the flow of signaling information and are therefore "bottlenecks", representing central points for communication in an interaction network.[52] Previously, proteins with high betweenness have been implicated in crucial roles in HCV infection and pathogenesis.[53,54] To investigate if NS5A preferentially targets bottlenecks (defined as the top 10% of the nodes in the HPI ranked by betweenness), we estimated the fraction of NS5A interactors that were bottlenecks in the HPI. A significant proportion (39 of 108; 36.1%) of the NS5A interactors were identified as bottlenecks in the HPI (Supporting Information, Table S6); this number is significantly higher than the number of bottlenecks among randomly selected nodes (10.72 ± 3.17 with $p < 0.001$; Figure 1D; see Supporting Information). These include growth factor receptor-binding protein 2 (GRB2), which plays an important role in the subversion of host signaling pathways by NS5A;[55] tumor protein 53 (TP53), a key mediator of the oncogenic effect of NS5A in HCV-induced HCC;[56] and tyrosine kinase SRC, which regulates the formation of NS5A-containing HCV replication complex.[57] Among the NS5A interacting proteins identified by our Y2H screening, ITSN1, an endocytic traffic associated protein, and GABARAPL2, an autophagy associated protein, were identified as network bottlenecks.

Our observations therefore suggest that NS5A preferentially interacts with highly central proteins in the host protein interactome; these interactions may help the virus to regulate efficiently the flow of the infection-related information in the host cellular network and manipulate the host metabolic machinery for its own survival and pathogenesis. Our observations are consistent with studies that suggested that viral pathogens tend to interact with well-connected host proteins that are central to the host cellular networks, thus enabling them to appropriate essential cellular functions.[21,22,26,58,59]

Functional Analysis of NS5A Interaction Network

Next, we investigated the NS5A infection network for the enrichment of specific biological associations (KEGG pathways, CATH structural domains; GO terms and Reactome Pathways; Supporting Information, Tables S7a, S7b, S7c and S7d). Notably, a significant proportion of the proteins in the NS5A infection network were mapped to the CATH Phosphorylase Kinase; domain 1, domain (CATH:3.30.200.20; 138 out of 1442, $p = 2.61 \times 10^{-45}$) including 23 of the 132 NS5A interacting host proteins ($p = 3.38 \times 10^{-14}$) (13 of which are bottlenecks in the HPI), based on the Gene3D protein domain assignments (Supporting Information, Table S7b). These include two novel interactions between EPHB6 (a kinase deficient receptor) and MAP4K4 and NS5A, identified by our Y2H assay (Table 1). The significant representation of cellular kinases in the NS5A infection network is consistent with the key roles played by reversible phosphorylation of NS5A in modulating various NS5A functions in HCV pathogenesis. Impairing NS5A hyperphosphorylation has been shown to inhibit HCV replication, and thus, the cellular kinases that regulate NS5A phosphorylation are important targets for anti-HCV therapy.[9,60−63]

The analysis of NS5A infection network revealed an enrichment of 79 KEGG pathways (Supporting Information, Table S7a). Furthermore, 31 of the 39 NS5A interacting bottlenecks (hereafter referred to as bottlenecks) were mapped to 75 of the 79 enriched KEGG pathways (Supporting Information, Table S5). Among the 75 bottleneck-associated enriched KEGG pathways, the highest numbers were associated with various cancers and infectious diseases (31 enriched KEGG pathways; 27 bottlenecks), followed by immune system, signal transduction and endocrine system (23 enriched KEGG pathways; 27 bottlenecks), cell growth and death (4 enriched KEGG pathways; 9 bottlenecks), nervous system (4 enriched KEGG pathways; 8 bottlenecks) and cellular communication (3 enriched KEGG pathways; 14 bottlenecks) among others (Tables 2, S8a, Supporting Information). Below we describe our observations on the most prominent enriched biological themes of interest that were associated with the NS5A infection network, with a specific focus on the bottlenecks.

Cancers and Infectious Diseases

The analysis of the NS5A interaction network revealed that NS5A specifically targets host factors that participate in various complex human diseases. Thirty-four NS5A interactors including 24 bottlenecks were mapped to one or more of the 17 enriched KEGG pathways associated with different infectious diseases (Supporting Information, Tables S7a, S8a). Among the most prominent associations, 12 bottlenecks were mapped to "Epstein−Barr virus infection" ($p = 1.36 \times 10^{-27}$); 10 to "Hepatitis C" ($p = 3.47 \times 10^{-24}$); 10 to "HTLV-I infection" ($p = 1.39 \times 10^{-20}$); 9 to "Hepatitis B" ($p = 3.33 \times 10^{-26}$); 8 to "Measles" ($p = 5.69 \times 10^{-17}$); 7 bottlenecks were mapped to "Influenza A" ($p = 5.01 \times 10^{-12}$); 7 to "Herpes simplex infection" ($p = 1.47 \times 10^{-13}$) and 6 to "Tuberculosis" ($p = 3.02 \times 10^{-6}$) (Supporting Information, Tables S7a, S8a). These associations include infectious diseases induced by various bacterial and viral pathogens thereby suggesting that HCV and other pathogens may systematically target specific host factors, the perturbation of which may contribute to the onset of various human diseases.

Also, 19 bottlenecks were mapped to one or more of the 16 enriched KEGG pathways associated with various cancers. Among the most prominent associations, 10 bottlenecks were mapped to "Viral carcinogenesis" ($p = 1.3 \times 10^{-30}$); 8 each were mapped to "Prostrate cancer" ($p = 4.27 \times 10^{-25}$), "Endometrial cancer" ($p = 5.52 \times 10^{-21}$) and "Colorectal cancer" ($p = 4.22 \times 10^{-18}$); 7 to "Pancreatic cancer" ($p = 1.94 \times 10^{-18}$); 6 to "Chronic myeloid leukemia" ($p = 1.61 \times 10^{-30}$) and 5 each to "Non-small cell lung cancer" ($p = 8.66 \times 10^{-15}$) and "Glioma" ($p = 2.38 \times 10^{-14}$) (Supporting Information, Tables S7a, S8a). The significant association of HCV with host factors central to various cancer pathways (including tumor suppressors such as TP53) is consistent with previous observations that viral pathogens significantly targeted host proteins associated with cancer pathways,[59,64,65] which likely plays major roles in tumorigenesis.

Immune System and Signal Transduction

HCV infection induces various active and passive host immune responses including the recognition of viral RNA by host cell receptors. These events lead to the production of Type I interferons (IFN-α/β) and inflammatory cytokines in the infected hepatocytes, initiating the antiviral response. HCV persistence in the host is determined by the virus's ability to impair host immune responses.[66−69]

The analysis of the NS5A interaction network revealed that 21 of the 132 NS5A interacting proteins, including 16 bottlenecks and their interacting partners, were mapped to one or more enriched KEGG pathways associated with the immune system (Supporting Information, Tables S7a, S8a).

Table 2. KEGG Pathway Functional Categories (Subclasses) Sorted by the Number of Enriched Pathways (≥3) Associated with One or More NS5A Interacting Bottlenecks

category	no. of enriched pathways	no. of bottlenecks	associated bottlenecks	KEGG pathways in the given category associated with most number of bottlenecks
infectious diseases	16	24	ACTB, AKT1, CDK1, CSNK2A1, CTNNB1, FLNA, FYN, GPS2, GRB2, GSK3B, HSPB1, JAK1, LCK, LYN, PIK3R1, PPP2CA, RAF1, SRC, STAT1, SYK, TBP, TGFBR1, TP53, TRAF2	"Epstein−Barr virus infection"; "HTLV-I infection"; "Hepatitis C"; "Hepatitis B"; "Measles"; "Influenza A"; "Herpes simplex infection"; "Tuberculosis"; "Toxoplasmosis"; "Chagas disease (American trypanosomiasis)"; "Bacterial invasion of epithelial cells"
cancers	16	19	AKT1, AXIN1, CDK1, CTNNB1, GRB2, GSK3B, HSP90AA1, JAK1, LYN, RAF1, SRC, STAT1, SYK, TBP, TGFBR1, THBS1, TP53, TRAF2	"Pathways in cancer"; "Viral carcinogenesis"; "Prostate cancer"; "Endometrial cancer"; "Colorectal cancer"; "Pancreatic cancer"; "Chronic myeloid leukemia"; "Non-small cell lung cancer"; "Glioma"; "Small cell lung cancer"; "Renal cell carcinoma"; "Melanoma"; "Acute myeloid leukemia"
immune system	10	16	ACTB, AKT1, CTNNB1, FYN, GRB2, GSK3B, HSP90AA1, LCK, LYN, PIK3R1, PIN1, RAF1, SRC, STAT1, SYK, TRAF	"Chemokine signaling pathway"; "T cell receptor signaling pathway"; "Fc epsilon RI signaling pathway"; "B cell receptor signaling pathway"; "Natural killer cell mediated cytotoxicity"; "Fc gamma R-mediated phagocytosis"
signal transduction	9	22	AKT1, AXIN1, CSKN1A1, CTNNB1, FLN, GRB2, GSK3B, HSP90AA1, HSPB1, JAK1, LCK, LYN, PIK3R1, PPP2CA, RAF1, SRC, STAT1, SYK, TGFBR1, THBS1, TP53, TRAF2	"PI3K-Akt signaling pathway"; "MAPK signaling pathway"; "Wnt signaling pathway"; "ErbB signaling pathway"; "VEGF signaling pathway"; "NF-kappa B signaling pathway"; "Jak-STAT signaling pathway"
nervous system	5	8	AKT1, GRB2, GSK3B, LYN, PIK3R1, PPP2CA, RAF1, TP53	"Neurotrophin signaling pathway"; "Long-term depression"; "Dopaminergic synapse"; "Long-term potentiation"
endocrine system	4	10	AKT1, CDK1, GRB2, GSK3B, HSP90AA1, PIK3R1, PLK1, RAF1, SRC, TRAF2	"Progesterone-mediated oocyte maturation"; "Insulin signaling pathway"; "GnRH signaling pathway"; "Adipocytokine signaling pathway"
cell growth and death	4	9	AKT1, CDK1, GSK3B, PIK3R1, PLK1, PPP2CA, THBS1, TP53, TRAF2	"Cell cycle"; "Apoptosis"; "p53 signaling pathway"; "Oocyte meiosis"
cell communication	3	14	ACTB, AKT1, CSNK2A1, CTNNB1, FLNA, FYN, GRB2, GSK3B, PIK3R1, PPP2CA, RAF1, SRC, TGFBR1, THBS1	"Focal adhesion"; "Tight junction"; "Adherens junction"
development	3	12	AKT1, FHL2, FYN, GRB2, GSK3B, JAK1, LCK, PIK3R1, STAT1, SYK, TGFBR1, THBS1	"Osteoclast differentiation"; "Axon guidance"; "Dorso-ventral axis formation"

Eight bottlenecks were mapped to the enriched KEGG pathway "Chemokine signaling pathway" ($p = 2.27 \times 10^{-10}$), which is consistent with the modulation of host interferon signaling by NS5A in HCV infection.[70] In addition, 7 bottlenecks each were mapped to "T cell receptor signaling pathway" ($p = 4.6 \times 10^{-24}$), "Fc epsilon RI signaling pathway" ($p = 2.86 \times 10^{-14}$) and "B cell receptor signaling pathway" ($p = 1.8 \times 10^{-14}$) and 6 bottlenecks were mapped to "Natural killer cell mediated cytotoxicity" ($p = 1.92 \times 10^{-12}$). Three bottlenecks (AKT1, PIK3R1 and STAT1) were also mapped to the enriched KEGG pathway "Toll-like receptor signaling pathway" ($p = 3.23 \times 10^{-7}$; Supporting Information, Tables S7a, S8a). Toll-like receptor 3 mediated chemokine and cytokine signaling plays an important role in the host immune response in HCV infection.[71] Therefore, NS5A interaction with bottlenecks, which function in various aspects of the host immune response, may significantly contribute to the perturbation of the host immune system in HCV pathogenesis.

Additionally, 32 of 132 NS5A interacting proteins examined in the present study, including 24 bottlenecks, were mapped to various pathways associated with the signal transduction and the endocrine system (Supporting Information, Tables S7a, S8a), many of which are implicated in HCV infection and HCC progression and are targets for molecular therapy in HCC.[22,72−74]

Eleven bottlenecks were mapped to the enriched KEGG pathway "PI3K-Akt signaling pathway" ($p = 2.2 \times 10^{-24}$; Supporting Information, Tables S7a, S8a), which is consistent with a previous study that NS5A stimulates the activation of PI3K-Akt pathway, which contributes to HCC in HCV infection.[75] Eight bottlenecks were mapped to the enriched KEGG pathway "MAPK signaling pathway" ($p = 2.4 \times 10^{-19}$; Supporting Information, Tables S7a, S8a). Elements of the MAPK signaling cascades are directly involved in the progression of HCV infection, particularly in association with HCV Core and E2 proteins,[22,24,76,77] thereby suggesting that NS5A interactions with the key facilitators of MAPK signaling in the host interactome may play an important role in regulating the reversible phosphorylation of NS5A and may contribute to the progression of HCV pathogenesis.

Bottlenecks AKT1, GRB2, GSK3B, PIK3R1 and RAF1 and many of their interactors were mapped to the enriched KEGG pathway "Insulin signaling pathway" ($p = 2.42 \times 10^{-13}$; Supporting Information, Tables S7a, S8a); these proteins are highlighted in Figure 2. Insulin signaling plays an important role in regulating glucose and lipid metabolism, and the disruption of this process may contribute to insulin resistance (IR). IR is linked with steatosis, fibrosis progression and poor interferon-α response in HCV infection.[78−80] Suppression of AKT1 and GSK3B activity in HCV infection disrupts glucose metabolism and contributes to IR.[81,82] Furthermore, PIK3R1 and NS5A interactor PIK3CB (Figure 2) are subunits of phosphatidylinositol 3-kinase (PI3K), which controls insulin secretion;[83] PI3K also facilitates the activation of the proto-oncogene beta-catenin (CTNNB1) by NS5A, which contributes to the development of HCC in HCV pathogenesis.[84] Previously, HCV Core protein has been directly implicated in the induction of IR in HCV infection,[85] while there is little evidence suggesting definitive links between NS5A and IR. Our observations, however, suggest that NS5A directly interacts with key regulators of insulin metabolism and may, therefore, play a major role in modulating HCV-induced IR and eventually HCC.

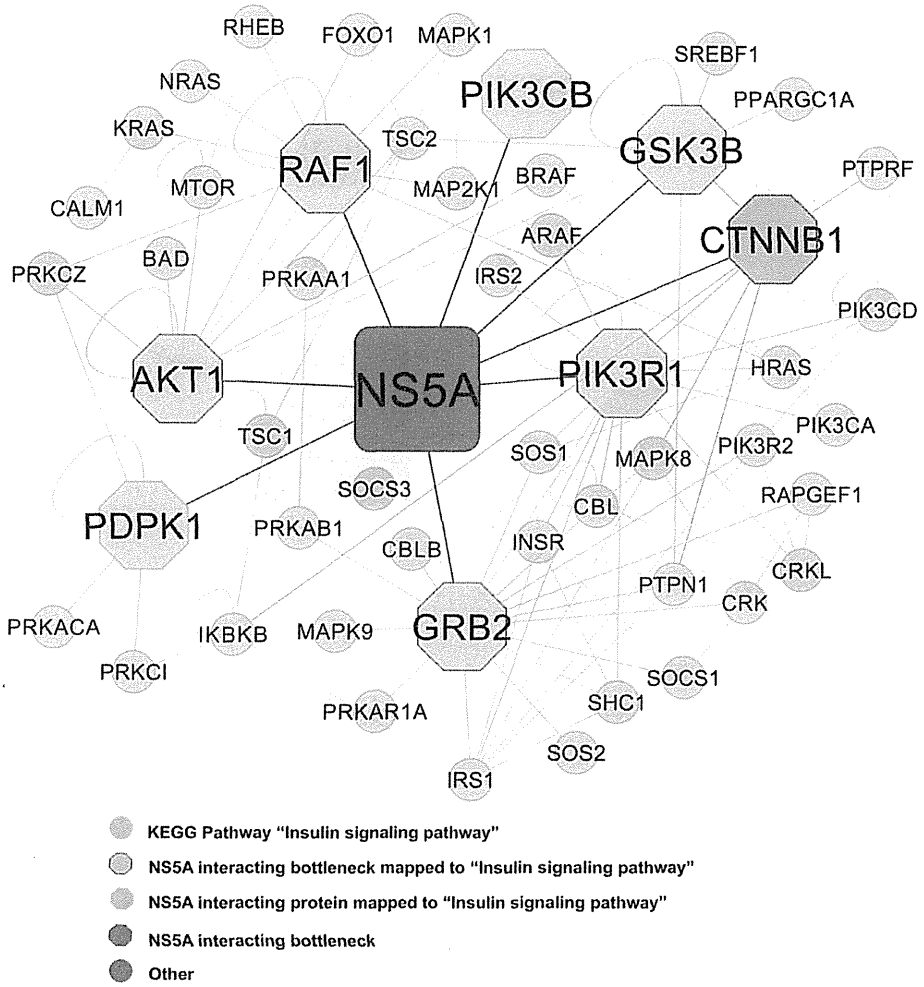

Figure 2. NS5A interacting bottlenecks and their interacting partners associated with the enriched KEGG pathway hsa04910: "Insulin signaling pathway".

Cell Adhesion and Communication

The perturbation of adherens and tight junction associated proteins has been implicated in HCV entry, cell–cell transmission and hepatoma migration in HCV infection.[86−88] In the NS5A infection network, eight bottlenecks (ACTB, AKT1, CSNK2A1, CTNNB1, FYN, PPP2CA, SRC and TGFBR1) were mapped to either or both of the enriched KEGG pathways "Adherens Junction" ($p = 1.03 \times 10^{-15}$) and "Tight junction" ($p = 1.19 \times 10^{-5}$), which are associated with cell adhesion junctions and cellular communication (Supporting Information, Tables S7a, S8a). CSNK2A1 is the catalytic (alpha) subunit of Casein Kinase II (CK2), which phosphorylates NS5A and regulates the production of infectious viral particles.[63] CTNNB1, a key component of cell-adhesion complexes, is positively regulated by CK2.[89] Furthermore, the activation of CTNNB1 by NS5A significantly contributes to HCC.[84] Taken together, our observations suggest that NS5A interactions with bottlenecks, which regulate cell–cell adhesion (CSNK2A1, CTNNB1) and cytoskeletal organization (ACTB), may significantly contribute to the progression of HCV life cycle and tumorigenesis in HCV pathogenesis.

Eleven bottlenecks were mapped to the enriched KEGG pathway "Focal Adhesion" ($p = 1.02 \times 10^{-17}$; Supporting Information, Tables S7a, S8a), thereby reiterating that focal adhesion is a major target of NS5A.[22] Focal adhesion regulates cell migration and adhesion, and some of its components were directly implicated in the regulation of HCV replication and propagation in our earlier study.[24] Our observations thus suggest that NS5A interactions with key components of the focal adhesion machinery may play important roles in the HCV lifecycle. For instance, NS5A interacts with bottleneck THBS1 (Thrombospondin-1), a glycoprotein, which was mapped to the KEGG "Focal Adhesion" pathway. THBS1 plays a key role in NS5A-mediated activation of the cytokine TGF-β1, which facilitates HCV replication and progressive liver fibrosis in HCV infection.[90] Our observations suggest that direct NS5A interactions with the bottlenecks THBS1 and TGFBR1 (TGF-β receptor 1; KEGG Pathway "Adherens Junction"), a key facilitator of TGF-β downstream signaling, may be crucial in facilitating HCV replication and tumorigenesis in HCV pathogenesis.

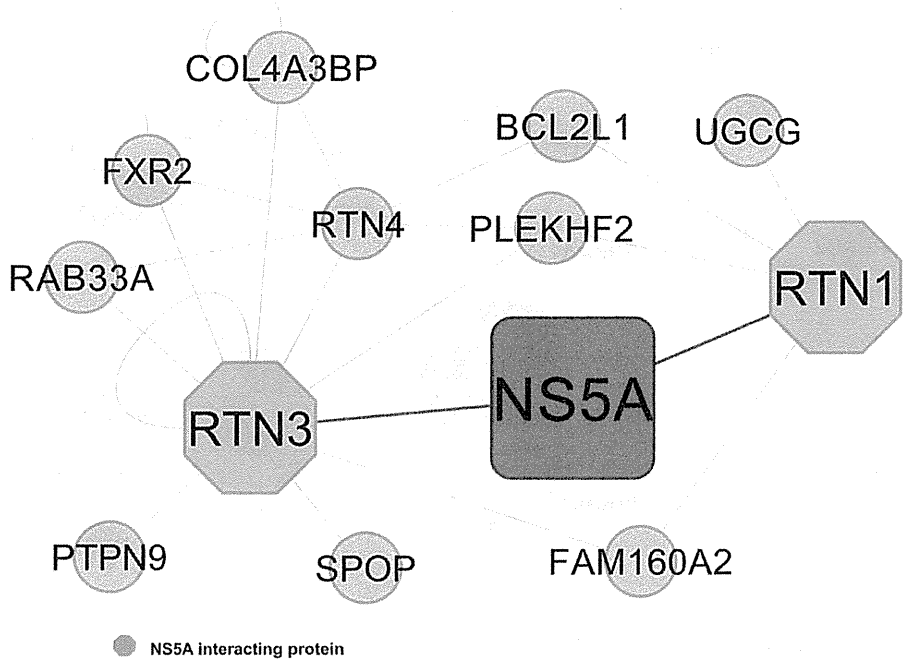

Figure 3. ER-localized host factors RTN1 and RTN3 were found to interact (blue edges) with NS5A in an Y2H screening of human liver cDNA library using NS5A as bait.

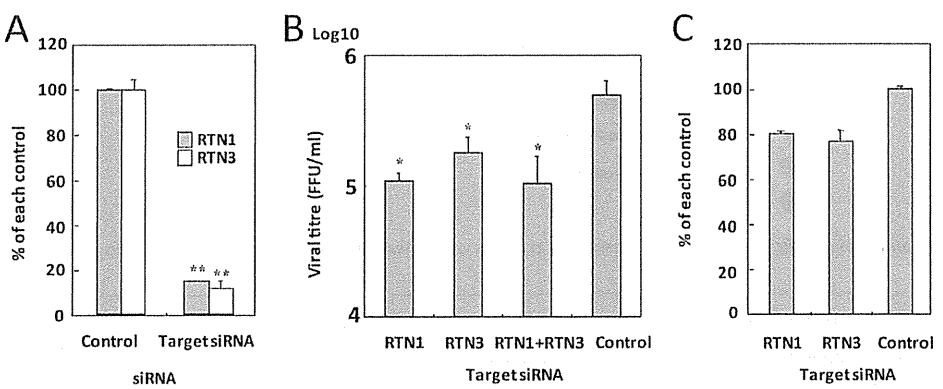

Figure 4. Effects of knockdown of RTN1 and RTN3 on HCV propagation and replication. Host factors RTN1 and RTN3 were suppressed by RNAi (A) in Huh7OK1 cells infected with HCV JFH1 strain (genotype 2a). The amounts of viral titer (B) and intracellular viral RNA (C) were estimated. Each value was represented as percentage of the cells transfected with the control siRNA. FFU: Focus-forming units; *: $p < 0.05$, **: $p < 0.01$.

Cellular Transport

Cellular factors associated with endocytic trafficking are key facilitators of the HCV life cycle, particularly HCV entry into the hepatic cells.[91−93] Endocytosis of the extracellular growth factor receptor (EGFR) in association with the cell surface glycoprotein CD81 plays a crucial role in HCV internalization and entry and is, therefore, an attractive target of anti-HCV strategies.[94] In the NS5A infection network, NS5A interactors ARAP1 and HSPA1A together with two bottlenecks (SRC, TGFBR1) were mapped to the enriched KEGG pathway "Endocytosis" ($p = 2.97 \times 10^{-8}$; Supporting Information, Tables S7a, S8a). ARAP1, a Golgi associated protein, negatively regulates EGFR trafficking, and decreased ARAP1 expression contributes to enhanced EGFR endocytosis.[95] Therefore, NS5A interaction with ARAP1 may facilitate EGFR internalization and thus viral entry in HCV infection.

NS5A Interacting Host Proteins RTN1 and RTN3 Function in HCV Propagation but Not Replication

Traditionally, viral and host proteins associated with the HCV lifecycle (internalization, replication, assembly and release) have been preferred targets in the anti-HCV studies. During infection, HCV localizes to the detergent-resistant membrane fraction (DRM) derived from the ER, where the viral replication and assembly take place.[4] Thus, of the novel interactions identified in our Y2H assay, we focused on two ER-localized host factors RTN1 and RTN3 (Figure 3). RTN1 and RTN3 belong to a group of proteins named Reticulons, which are integral to maintaining the shape and organization of the

ER and have been implicated in facilitating the replication of various positive-strand RNA viruses.[96−98] Furthermore, both RTN1 and RTN3 have been specifically detected in the very low density lipoprotein (VLDL) transport vesicle (VTV);[99] VTV is a key component of the VLDL secretory pathway, which plays an essential role in the production and the release of the infectious HCV particles.[100] Therefore, NS5A interactions with RTN1 and RTN3 suggested novel and potentially crucial roles of the two host proteins in the replication and/or release stages of the HCV lifecycle.

We performed cellular assays to assess the impact of RTN1 and RTN3 siRNA knockdowns on HCV replication and release. Since the HCV-production systems using the HCV JFH1 infectious strain (genotype 2a) isolates alone are capable of both efficient replication and the production of the infectious HCV particles, JFH1 was used to infect the Huh7OK1 cell line 24h after transfection with each siRNA (see Materials and Methods). The infected cells were harvested after 72 h postinfection, and the expression of each host protein was assessed by qRT-PCR (Figure 4A). The viral titer was significantly decreased by individual and double knockdowns of RTN1 and RTN3 (Figure 4B). However, RTN1 and RTN3 knockdowns had no effect on the intracellular viral RNA levels in the HCV infected cells (Figure 4C), suggesting that RTN1 and RTN3 regulate HCV propagation but not HCV replication.

CONCLUSIONS

We describe here our observations of PPIs between HCV NS5A and host proteins. By employing a multifold approach involving an experimental Y2H assay and literature mining, we derived a comprehensive set of experimentally determined binary interactions between NS5A and host proteins. We proceeded to map the combined NS5A−host interactions onto an overall interaction network, which comprised a repertoire of connections, which potentially enable NS5A to link up with and modulate the components of the host cellular networks. We then employed a network-based approach to understand the biological context of these connections in HCV pathogenesis with the help of the TargetMine data warehouse.

A functional analysis of the PPI networks highlighted NS5A interactions with several well connected host factors (hubs) and centrally located "bottlenecks" in the host cellular networks that function in cellular pathways associated with immune system and cell signaling, cellular adhesion and cell transport, cell growth and cell death and ER homeostasis among others. The "bottlenecks" include several proteins that were previously implicated in HCV pathogenesis, thereby suggesting that NS5A interactions with centrally connected host factors may enable the virus to influence strongly the host cellular processes in HCV infection. Notably, many bottlenecks were mapped to pathways associated with the infectious diseases induced by diverse bacterial and viral pathogens of the human host. These observations thus suggest the presence of some common themes underlying the onset of various human diseases associated with pathogenic infection in humans, a better understanding of which may be helpful in optimizing broad spectrum approaches to counteracting a wide range of pathogenic infections.

Cellular assays based on siRNA knockdowns in the HCV infected and replicon cells demonstrated RTN1 and RTN3, ER-localized NS5A interacting proteins, to be novel regulators of HCV propagation, but not replication, and thus promising novel candidates for anti-HCV therapy.

Our analysis therefore provides further insights into the role of NS5A−host interactions in HCV infection, a deeper understanding of which may aid in the identification of new clinically relevant targets for optimizing the therapeutic strategies to manipulate HCV−host interactions and thus more effectively combating HCV infection. Our analysis also emphasizes the importance of elaborate network-based computational approaches that integrate diverse biological data types in investigating host−pathogen interactions.

ASSOCIATED CONTENT

Supporting Information

Supporting methods, figures, and tables. This material is available free of charge via the Internet at http://pubs.acs.org.

AUTHOR INFORMATION

Corresponding Author

*E-mail: kenji@nibio.go.jp (K.M.); lokesh@nibio.go.jp (L.P.T.). Tel: +81-72-641-9890. Fax: +81-72-641-9881.

Author Contributions

‖L. P. Tripathi and H. Kambara contributed equally to this work.

Notes

The authors declare no competing financial interest.

ACKNOWLEDGMENTS

This study was supported by the Industrial Technology Research Grant Program in 2007 from New Energy and Industrial Technology Development Organization (NEDO) of Japan and also by grants-in-aid from the Ministry of Health, Labor, and Welfare; the Ministry of Education, Culture, Sports, Science, and Technology; the Osaka University Global Center of Excellence Program; and the Foundation for Biomedical Research and Innovation.

REFERENCES

(1) Dubuisson, J. Hepatitis C virus proteins. *World J. Gastroenterol.* **2007**, *13* (17), 2406−15.

(2) Moriishi, K.; Matsuura, Y. Host factors involved in the replication of hepatitis C virus. *Rev. Med. Virol.* **2007**, *17* (5), 343−54.

(3) Myrmel, H.; Ulvestad, E.; Asjo, B. The hepatitis C virus enigma. *APMIS* **2009**, *117* (5−6), 427−39.

(4) Tang, H.; Grise, H. Cellular and molecular biology of HCV infection and hepatitis. *Clin. Sci.* **2009**, *117* (2), 49−65.

(5) Pol, S.; Vallet-Pichard, A.; Corouge, M.; Mallet, V. O. Hepatitis C: epidemiology, diagnosis, natural history and therapy. *Contrib. Nephrol.* **2012**, *176*, 1−9.

(6) Kuiken, C.; Simmonds, P. Nomenclature and numbering of the hepatitis C virus. *Methods Mol. Biol.* **2009**, *510*, 33−53.

(7) Moradpour, D.; Penin, F.; Rice, C. M. Replication of hepatitis C virus. *Nat. Rev. Microbiol.* **2007**, *5* (6), 453−63.

(8) Love, R. A.; Brodsky, O.; Hickey, M. J.; Wells, P. A.; Cronin, C. N. Crystal structure of a novel dimeric form of NS5A domain I protein from hepatitis C virus. *J. Virol.* **2009**, *83* (9), 4395−403.

(9) Yamasaki, L. H.; Arcuri, H. A.; Jardim, A. C.; Bittar, C.; de Carvalho-Mello, I. M.; Rahal, P. New insights regarding HCV-NS5A structure/function and indication of genotypic differences. *Virol. J.* **2012**, *9*, 14.

(10) Appel, N.; Zayas, M.; Miller, S.; Krijnse-Locker, J.; Schaller, T.; Friebe, P.; Kallis, S.; Engel, U.; Bartenschlager, R. Essential role of domain III of nonstructural protein 5A for hepatitis C virus infectious particle assembly. *PLoS Pathog.* **2008**, *4* (3), e1000035.

(11) Gale, M. J., Jr.; Korth, M. J.; Tang, N. M.; Tan, S. L.; Hopkins, D. A.; Dever, T. E.; Polyak, S. J.; Gretch, D. R.; Katze, M. G. Evidence that hepatitis C virus resistance to interferon is mediated through repression of the PKR protein kinase by the nonstructural 5A protein. *Virology* **1997**, *230* (2), 217–27.
(12) Ghosh, S.; Ahrens, W. A.; Phatak, S. U.; Hwang, S.; Schrum, L. W.; Bonkovsky, H. L. Association of filamin A and vimentin with hepatitis C virus proteins in infected human hepatocytes. *J. Viral Hepatitis* **2011**, *18* (10), e568–77.
(13) Gao, M.; Nettles, R. E.; Belema, M.; Snyder, L. B.; Nguyen, V. N.; Fridell, R. A.; Serrano-Wu, M. H.; Langley, D. R.; Sun, J. H.; O'Boyle, D. R., 2nd; Lemm, J. A.; Wang, C.; Knipe, J. O.; Chien, C.; Colonno, R. J.; Grasela, D. M.; Meanwell, N. A.; Hamann, L. G. Chemical genetics strategy identifies an HCV NS5A inhibitor with a potent clinical effect. *Nature* **2010**, *465* (7294), 96–100.
(14) Lee, C. Discovery of hepatitis C virus NS5A inhibitors as a new class of anti-HCV therapy. *Arch. Pharmacal Res.* **2011**, *34* (9), 1403–7.
(15) Lemm, J. A.; O'Boyle, D., 2nd; Liu, M.; Nower, P. T.; Colonno, R.; Deshpande, M. S.; Snyder, L. B.; Martin, S. W.; St Laurent, D. R.; Serrano-Wu, M. H.; Romine, J. L.; Meanwell, N. A.; Gao, M. Identification of hepatitis C virus NS5A inhibitors. *J. Virol.* **2010**, *84* (1), 482–91.
(16) Lemon, S. M.; McKeating, J. A.; Pietschmann, T.; Frick, D. N.; Glenn, J. S.; Tellinghuisen, T. L.; Symons, J.; Furman, P. A. Development of novel therapies for hepatitis C. *Antiviral Res.* **2010**, *86* (1), 79–92.
(17) Fusco, D. N.; Chung, R. T. Novel therapies for hepatitis C: insights from the structure of the virus. *Annu. Rev. Med.* **2012**, *63*, 373–87.
(18) Buhler, S.; Bartenschlager, R. New targets for antiviral therapy of chronic hepatitis C. *Liver Int.* **2012**, *32* (Suppl 1), 9–16.
(19) Sarrazin, C.; Hezode, C.; Zeuzem, S.; Pawlotsky, J. M. Antiviral strategies in hepatitis C virus infection. *J. Hepatol.* **2012**, *56* (Suppl), S88–S100.
(20) Wang, S.; Wu, X.; Pan, T.; Song, W.; Wang, Y.; Zhang, F.; Yuan, Z. Viperin inhibits hepatitis C virus replication by interfering with binding of NS5A to host protein hVAP-33. *J. Gen. Virol.* **2012**, *93* (Pt1), 83–92.
(21) Durmus Tekir, S.; Cakir, T.; Ulgen, K. O. Infection strategies of bacterial and viral pathogens through pathogen-human protein-protein interactions. *Front. Microbiol.* **2012**, *3*, 46.
(22) de Chassey, B.; Navratil, V.; Tafforeau, L.; Hiet, M. S.; Aublin-Gex, A.; Agaugue, S.; Meiffren, G.; Pradezynski, F.; Faria, B. F.; Chantier, T.; Le Breton, M.; Pellet, J.; Davoust, N.; Mangeot, P. E.; Chaboud, A.; Penin, F.; Jacob, Y.; Vidalain, P. O.; Vidal, M.; Andre, P.; Rabourdin-Combe, C.; Lotteau, V. Hepatitis C virus infection protein network. *Mol. Syst. Biol.* **2008**, *4*, 230.
(23) Tan, S. L.; Ganji, G.; Paeper, B.; Proll, S.; Katze, M. G. Systems biology and the host response to viral infection. *Nat. Biotechnol.* **2007**, *25* (12), 1383–9.
(24) Tripathi, L. P.; Kataoka, C.; Taguwa, S.; Moriishi, K.; Mori, Y.; Matsuura, Y.; Mizuguchi, K. Network based analysis of hepatitis C virus Core and NS4B protein interactions. *Mol. BioSyst.* **2010**, *6* (12), 2539–53.
(25) Friedel, C. C.; Haas, J. Virus-host interactomes and global models of virus-infected cells. *Trends Microbiol.* **2011**, *19* (10), 501–8.
(26) Tafforeau, L.; Rabourdin-Combe, C.; Lotteau, V. Virus-human cell interactomes. *Methods Mol. Biol.* **2012**, *812*, 103–20.
(27) Aizaki, H.; Aoki, Y.; Harada, T.; Ishii, K.; Suzuki, T.; Nagamori, S.; Toda, G.; Matsuura, Y.; Miyamura, T. Full-length complementary DNA of hepatitis C virus genome from an infectious blood sample. *Hepatology* **1998**, *27* (2), 621–7.
(28) Hamamoto, I.; Nishimura, Y.; Okamoto, T.; Aizaki, H.; Liu, M.; Mori, Y.; Abe, T.; Suzuki, T.; Lai, M. M.; Miyamura, T.; Moriishi, K.; Matsuura, Y. Human VAP-B is involved in hepatitis C virus replication through interaction with NS5A and NS5B. *J. Virol.* **2005**, *79* (21), 13473–82.
(29) Rebholz-Schuhmann, D.; Kirsch, H.; Arregui, M.; Gaudan, S.; Riethoven, M.; Stoehr, P. EBIMed—text crunching to gather facts for proteins from Medline. *Bioinformatics* **2007**, *23* (2), e237–44.
(30) Rebholz-Schuhmann, D.; Arregui, M.; Gaudan, S.; Kirsch, H.; Jimeno, A. Text processing through Web services: calling Whatizit. *Bioinformatics* **2008**, *24* (2), 296–8.
(31) Stark, C.; Breitkreutz, B. J.; Reguly, T.; Boucher, L.; Breitkreutz, A.; Tyers, M. BioGRID: a general repository for interaction datasets. *Nucleic Acids Res.* **2006**, *34* (Database issue), D535–9.
(32) Turner, B.; Razick, S.; Turinsky, A. L.; Vlasblom, J.; Crowdy, E. K.; Cho, E.; Morrison, K.; Donaldson, I. M.; Wodak, S. J. iRefWeb: interactive analysis of consolidated protein interaction data and their supporting evidence. *Database* **2010**, *2010*, baq023.
(33) Chen, Y. A.; Tripathi, L. P.; Mizuguchi, K. TargetMine, an integrated data warehouse for candidate gene prioritisation and target discovery. *PLoS One* **2011**, *6* (3), e17844.
(34) Cline, M. S.; Smoot, M.; Cerami, E.; Kuchinsky, A.; Landys, N.; Workman, C.; Christmas, R.; Avila-Campilo, I.; Creech, M.; Gross, B.; Hanspers, K.; Isserlin, R.; Kelley, R.; Killcoyne, S.; Lotia, S.; Maere, S.; Morris, J.; Ono, K.; Pavlovic, V.; Pico, A. R.; Vailaya, A.; Wang, P. L.; Adler, A.; Conklin, B. R.; Hood, L.; Kuiper, M.; Sander, C.; Schmulevich, I.; Schwikowski, B.; Warner, G. J.; Ideker, T.; Bader, G. D. Integration of biological networks and gene expression data using Cytoscape. *Nat. Protoc.* **2007**, *2* (10), 2366–82.
(35) Smoot, M. E.; Ono, K.; Ruscheinski, J.; Wang, P. L.; Ideker, T. Cytoscape 2.8: new features for data integration and network visualization. *Bioinformatics* **2011**, *27* (3), 431–2.
(36) Assenov, Y.; Ramirez, F.; Schelhorn, S. E.; Lengauer, T.; Albrecht, M. Computing topological parameters of biological networks. *Bioinformatics* **2008**, *24* (2), 282–4.
(37) Lees, J.; Yeats, C.; Perkins, J.; Sillitoe, I.; Rentzsch, R.; Dessailly, B. H.; Orengo, C. Gene3D: a domain-based resource for comparative genomics, functional annotation and protein network analysis. *Nucleic Acids Res.* **2012**, *40* (Database issue), D465–71.
(38) Ashburner, M.; Ball, C. A.; Blake, J. A.; Botstein, D.; Butler, H.; Cherry, J. M.; Davis, A. P.; Dolinski, K.; Dwight, S. S.; Eppig, J. T.; Harris, M. A.; Hill, D. P.; Issel-Tarver, L.; Kasarskis, A.; Lewis, S.; Matese, J. C.; Richardson, J. E.; Ringwald, M.; Rubin, G. M.; Sherlock, G. Gene ontology: tool for the unification of biology. The Gene Ontology Consortium. *Nat. Genet.* **2000**, *25* (1), 25–9.
(39) Aoki-Kinoshita, K. F.; Kanehisa, M. Gene annotation and pathway mapping in KEGG. *Methods Mol. Biol.* **2007**, *396*, 71–91.
(40) Benjamini, Y.; Hochberg, Y. Controlling the false discovery rate—A practical and powerful approach to multiple testing. *J. R. Stat. Soc. B* **1995**, *57* (1), 289–300.
(41) Noble, W. S. How does multiple testing correction work? *Nat. Biotechnol.* **2009**, *27* (12), 1135–7.
(42) Okamoto, K.; Mori, Y.; Komoda, Y.; Okamoto, T.; Okochi, M.; Takeda, M.; Suzuki, T.; Moriishi, K.; Matsuura, Y. Intramembrane processing by signal peptide peptidase regulates the membrane localization of hepatitis C virus core protein and viral propagation. *J. Virol.* **2008**, *82* (17), 8349–61.
(43) Okamoto, T.; Omori, H.; Kaname, Y.; Abe, T.; Nishimura, Y.; Suzuki, T.; Miyamura, T.; Yoshimori, T.; Moriishi, K.; Matsuura, Y. A single-amino-acid mutation in hepatitis C virus NS5A disrupting FKBP8 interaction impairs viral replication. *J. Virol.* **2008**, *82* (7), 3480–9.
(44) Wakita, T.; Pietschmann, T.; Kato, T.; Date, T.; Miyamoto, M.; Zhao, Z.; Murthy, K.; Habermann, A.; Krausslich, H. G.; Mizokami, M.; Bartenschlager, R.; Liang, T. J. Production of infectious hepatitis C virus in tissue culture from a cloned viral genome. *Nat. Med.* **2005**, *11* (7), 791–6.
(45) Taguwa, S.; Kambara, H.; Omori, H.; Tani, H.; Abe, T.; Mori, Y.; Suzuki, T.; Yoshimori, T.; Moriishi, K.; Matsuura, Y. Cochaperone activity of human butyrate-induced transcript 1 facilitates hepatitis C virus replication through an Hsp90-dependent pathway. *J. Virol.* **2009**, *83* (20), 10427–36.
(46) Kukihara, H.; Moriishi, K.; Taguwa, S.; Tani, H.; Abe, T.; Mori, Y.; Suzuki, T.; Fukuhara, T.; Taketomi, A.; Maehara, Y.; Matsuura, Y.

Human VAP-C negatively regulates hepatitis C virus propagation. *J. Virol.* **2009**, *83* (16), 7959–69.
(47) Nanda, S. K.; Herion, D.; Liang, T. J. The SH3 binding motif of HCV [corrected] NS5A protein interacts with Bin1 and is important for apoptosis and infectivity. *Gastroenterology* **2006**, *130* (3), 794–809.
(48) Liu, A. W.; Cai, J.; Zhao, X. L.; Jiang, T. H.; He, T. F.; Fu, H. Q.; Zhu, M. H.; Zhang, S. H. ShRNA-targeted MAP4K4 inhibits hepatocellular carcinoma growth. *Clin. Cancer Res.* **2011**, *17* (4), 710–20.
(49) Woodhouse, S. D.; Narayan, R.; Latham, S.; Lee, S.; Antrobus, R.; Gangadharan, B.; Luo, S.; Schroth, G. P.; Klenerman, P.; Zitzmann, N. Transcriptome sequencing, microarray, and proteomic analyses reveal cellular and metabolic impact of hepatitis C virus infection in vitro. *Hepatology* **2010**, *52* (2), 443–53.
(50) MacPherson, J. I.; Sidders, B.; Wieland, S.; Zhong, J.; Targett-Adams, P.; Lohmann, V.; Backes, P.; Delpuech-Adams, O.; Chisari, F.; Lewis, M.; Parkinson, T.; Robertson, D. L. An integrated transcriptomic and meta-analysis of hepatoma cells reveals factors that influence susceptibility to HCV infection. *PLoS One* **2011**, *6* (10), e25584.
(51) Yamashita, T.; Honda, M.; Kaneko, S. Molecular mechanisms of hepatocarcinogenesis in chronic hepatitis C virus infection. *J. Gastroenterol. Hepatol.* **2011**, *26* (6), 960–4.
(52) Yu, H.; Kim, P. M.; Sprecher, E.; Trifonov, V.; Gerstein, M. The importance of bottlenecks in protein networks: correlation with gene essentiality and expression dynamics. *PLoS Comput. Biol.* **2007**, *3* (4), e59.
(53) Rasmussen, A. L.; Diamond, D. L.; McDermott, J. E.; Gao, X.; Metz, T. O.; Matzke, M. M.; Carter, V. S.; Belisle, S. E.; Korth, M. J.; Waters, K. M.; Smith, R. D.; Katze, M. G. Systems virology identifies a mitochondrial fatty acid oxidation enzyme, dodecenoyl coenzyme A delta isomerase, required for hepatitis C virus replication and likely pathogenesis. *J. Virol.* **2011**, *85* (22), 11646–54.
(54) Diamond, D. L.; Krasnoselsky, A. L.; Burnum, K. E.; Monroe, M. E.; Webb-Robertson, B. J.; McDermott, J. E.; Yeh, M. M.; Dzib, J. F.; Susnow, N.; Strom, S.; Proll, S. C.; Belisle, S. E.; Purdy, D. E.; Rasmussen, A. L.; Walters, K. A.; Jacobs, J. M.; Gritsenko, M. A.; Camp, D. G.; Bhattacharya, R.; Perkins, J. D.; Carithers, R. L., Jr.; Liou, I. W.; Larson, A. M.; Benecke, A.; Waters, K. M.; Smith, R. D.; Katze, M. G. Proteome and computational analyses reveal new insights into the mechanisms of hepatitis C virus-mediated liver disease posttransplantation. *Hepatology* **2012**, *56* (1), 28–38.
(55) He, Y.; Nakao, H.; Tan, S. L.; Polyak, S. J.; Neddermann, P.; Vijaysri, S.; Jacobs, B. L.; Katze, M. G. Subversion of cell signaling pathways by hepatitis C virus nonstructural 5A protein via interaction with Grb2 and P85 phosphatidylinositol 3-kinase. *J. Virol.* **2002**, *76* (18), 9207–17.
(56) Jiang, Y. F.; He, B.; Li, N. P.; Ma, J.; Gong, G. Z.; Zhang, M. The oncogenic role of NS5A of hepatitis C virus is mediated by up-regulation of survivin gene expression in the hepatocellular cell through p53 and NF-kappaB pathways. *Cell Biol. Int.* **2011**, *35* (12), 1225–32.
(57) Pfannkuche, A.; Buther, K.; Karthe, J.; Poenisch, M.; Bartenschlager, R.; Trilling, M.; Hengel, H.; Willbold, D.; Haussinger, D.; Bode, J. G. c-Src is required for complex formation between the hepatitis C virus-encoded proteins NS5A and NS5B: a prerequisite for replication. *Hepatology* **2011**, *53* (4), 1127–36.
(58) Calderwood, M. A.; Venkatesan, K.; Xing, L.; Chase, M. R.; Vazquez, A.; Holthaus, A. M.; Ewence, A. E.; Li, N.; Hirozane-Kishikawa, T.; Hill, D. E.; Vidal, M.; Kieff, E.; Johannsen, E. Epstein-Barr virus and virus human protein interaction maps. *Proc. Natl. Acad. Sci. U. S. A.* **2007**, *104* (18), 7606–11.
(59) Pichlmair, A.; Kandasamy, K.; Alvisi, G.; Mulhern, O.; Sacco, R.; Habjan, M.; Binder, M.; Stefanovic, A.; Eberle, C. A.; Goncalves, A.; Burckstummer, T.; Muller, A. C.; Fauster, A.; Holze, C.; Lindsten, K.; Goodbourn, S.; Kochs, G.; Weber, F.; Bartenschlager, R.; Bowie, A. G.; Bennett, K. L.; Colinge, J.; Superti-Furga, G. Viral immune modulators perturb the human molecular network by common and unique strategies. *Nature* **2012**, *487* (7408), 486–90.
(60) Huang, H.; Jedynak, B. M.; Bader, J. S. Where have all the interactions gone? Estimating the coverage of two-hybrid protein interaction maps. *PLoS Comput. Biol.* **2007**, *3* (11), e214.
(61) Nordle Gilliver, A.; Griffin, S.; Harris, M. Identification of a novel phosphorylation site in hepatitis C virus NS5A. *J. Gen. Virol.* **2010**, *91* (Pt 10), 2428–32.
(62) Qiu, D.; Lemm, J. A.; O'Boyle, D. R., 2nd; Sun, J. H.; Nower, P. T.; Nguyen, V.; Hamann, L. G.; Snyder, L. B.; Deon, D. H.; Ruediger, E.; Meanwell, N. A.; Belema, M.; Gao, M.; Fridell, R. A. The effects of NS5A inhibitors on NS5A phosphorylation, polyprotein processing and localization. *J. Gen. Virol.* **2011**, *92* (Pt11), 2502–11.
(63) Tellinghuisen, T. L.; Foss, K. L.; Treadaway, J. Regulation of hepatitis C virion production via phosphorylation of the NS5A protein. *PLoS Pathog.* **2008**, *4* (3), e1000032.
(64) Chen, K. C.; Wang, T. Y.; Chan, C. H. Associations between HIV and human pathways revealed by protein-protein interactions and correlated gene expression profiles. *PLoS One* **2012**, *7* (3), e34240.
(65) Rozenblatt-Rosen, O.; Deo, R. C.; Padi, M.; Adelmant, G.; Calderwood, M. A.; Rolland, T.; Grace, M.; Dricot, A.; Askenazi, M.; Tavares, M.; Pevzner, S. J.; Abderazzaq, F.; Byrdsong, D.; Carvunis, A. R.; Chen, A. A.; Cheng, J.; Correll, M.; Duarte, M.; Fan, C.; Feltkamp, M. C.; Ficarro, S. B.; Franchi, R.; Garg, B. K.; Gulbahce, N.; Hao, T.; Holthaus, A. M.; James, R.; Korkhin, A.; Litovchick, L.; Mar, J. C.; Pak, T. R.; Rabello, S.; Rubio, R.; Shen, Y.; Singh, S.; Spangle, J. M.; Tasan, M.; Wanamaker, S.; Webber, J. T.; Roecklein-Canfield, J.; Johannsen, E.; Barabasi, A. L.; Beroukhim, R.; Kieff, E.; Cusick, M. E.; Hill, D. E.; Munger, K.; Marto, J. A.; Quackenbush, J.; Roth, F. P.; DeCaprio, J. A.; Vidal, M. Interpreting cancer genomes using systematic host network perturbations by tumour virus proteins. *Nature* **2012**, *487* (7408), 491–5.
(66) Barnaba, V. Hepatitis C virus infection: a "liaison a trois" amongst the virus, the host, and chronic low-level inflammation for human survival. *J. Hepatol.* **2010**, *53* (4), 752–61.
(67) Hiroishi, K.; Ito, T.; Imawari, M. Immune responses in hepatitis C virus infection and mechanisms of hepatitis C virus persistence. *J. Gastroenterol. Hepatol.* **2008**, *23* (10), 1473–82.
(68) Kawai, T.; Akira, S. Toll-like receptor and RIG-I-like receptor signaling. *Ann. N. Y. Acad. Sci.* **2008**, *1143*, 1–20.
(69) Sklan, E. H.; Charuworn, P.; Pang, P. S.; Glenn, J. S. Mechanisms of HCV survival in the host. *Nat. Rev. Gastroenterol. Hepatol.* **2009**, *6* (4), 217–27.
(70) Kang, S. M.; Won, S. J.; Lee, G. H.; Lim, Y. S.; Hwang, S. B. Modulation of interferon signaling by hepatitis C virus non-structural 5A protein: implication of genotypic difference in interferon treatment. *FEBS Lett.* **2010**, *584* (18), 4069–76.
(71) Li, K.; Li, N. L.; Wei, D.; Pfeffer, S. R.; Fan, M.; Pfeffer, L. M. Activation of chemokine and inflammatory cytokine response in hepatitis C virus-infected hepatocytes depends on Toll-like receptor 3 sensing of hepatitis C virus double-stranded RNA intermediates. *Hepatology* **2012**, *55* (3), 666–75.
(72) Tanaka, S.; Arii, S. Molecularly targeted therapy for hepatocellular carcinoma. *Cancer Sci.* **2009**, *100* (1), 1–8.
(73) Tanaka, S.; Arii, S. Current status of molecularly targeted therapy for hepatocellular carcinoma: basic science. *Int. J. Clin. Oncol.* **2010**, *15* (3), 235–41.
(74) Villanueva, A.; Chiang, D. Y.; Newell, P.; Peix, J.; Thung, S.; Alsinet, C.; Tovar, V.; Roayaie, S.; Minguez, B.; Sole, M.; Battiston, C.; Van Laarhoven, S.; Fiel, M. I.; Di Feo, A.; Hoshida, Y.; Yea, S.; Toffanin, S.; Ramos, A.; Martignetti, J. A.; Mazzaferro, V.; Bruix, J.; Waxman, S.; Schwartz, M.; Meyerson, M.; Friedman, S. L.; Llovet, J. M. Pivotal role of mTOR signaling in hepatocellular carcinoma. *Gastroenterology* **2008**, *135* (6), 1972–83.
(75) Cheng, D.; Zhao, L.; Zhang, L.; Jiang, Y.; Tian, Y.; Xiao, X.; Gong, G. p53 controls hepatitis C virus non-structural protein 5A-mediated downregulation of GADD45alpha expression via the NF-kappaB and PI3K-Akt pathways. *J. Gen. Virol.* **2013**, *94* (Pt 2), 326–35.
(76) Tripathi, L. P.; Kambara, H.; Moriishi, K.; Morita, E.; Abe, T.; Mori, Y.; Chen, Y. A.; Matsuura, Y.; Mizuguchi, K. Proteomic analysis

of hepatitis C virus (HCV) core protein transfection and host regulator PA28gamma knockout in HCV pathogenesis: a network-based study. *J. Proteome Res.* **2012**, *11* (7), 3664–79.
(77) Zhao, L. J.; Zhao, P.; Chen, Q. L.; Ren, H.; Pan, W.; Qi, Z. T. Mitogen-activated protein kinase signalling pathways triggered by the hepatitis C virus envelope protein E2: implications for the prevention of infection. *Cell Proliferation* **2007**, *40* (4), 508–21.
(78) Basaranoglu, M.; Basaranoglu, G. Pathophysiology of insulin resistance and steatosis in patients with chronic viral hepatitis. *World J. Gastroenterol.* **2011**, *17* (36), 4055–62.
(79) Del Campo, J. A.; Romero-Gomez, M. Steatosis and insulin resistance in hepatitis C: a way out for the virus? *World J. Gastroenterol.* **2009**, *15* (40), 5014–9.
(80) Douglas, M. W.; George, J. Molecular mechanisms of insulin resistance in chronic hepatitis C. *World J. Gastroenterol.* **2009**, *15* (35), 4356–64.
(81) Das, G. C.; Hollinger, F. B. Molecular pathways for glucose homeostasis, insulin signaling and autophagy in hepatitis C virus induced insulin resistance in a cellular model. *Virology* **2012**, *434* (1), 5–17.
(82) Miyamoto, H.; Moriishi, K.; Moriya, K.; Murata, S.; Tanaka, K.; Suzuki, T.; Miyamura, T.; Koike, K.; Matsuura, Y. Involvement of the PA28gamma-dependent pathway in insulin resistance induced by hepatitis C virus core protein. *J. Virol.* **2007**, *81* (4), 1727–35.
(83) Kaneko, K.; Ueki, K.; Takahashi, N.; Hashimoto, S.; Okamoto, M.; Awazawa, M.; Okazaki, Y.; Ohsugi, M.; Inabe, K.; Umehara, T.; Yoshida, M.; Kakei, M.; Kitamura, T.; Luo, J.; Kulkarni, R. N.; Kahn, C. R.; Kasai, H.; Cantley, L. C.; Kadowaki, T. Class IA phosphatidylinositol 3-kinase in pancreatic beta cells controls insulin secretion by multiple mechanisms. *Cell Metab.* **2010**, *12* (6), 619–32.
(84) Milward, A.; Mankouri, J.; Harris, M. Hepatitis C virus NS5A protein interacts with beta-catenin and stimulates its transcriptional activity in a phosphoinositide-3 kinase-dependent fashion. *J. Gen. Virol.* **2010**, *91* (Pt 2), 373–81.
(85) Alberstein, M.; Zornitzki, T.; Zick, Y.; Knobler, H. Hepatitis C core protein impairs insulin downstream signalling and regulatory role of IGFBP-1 expression. *J. Viral Hepatitis* **2012**, *19* (1), 65–71.
(86) Benedicto, I.; Molina-Jimenez, F.; Bartosch, B.; Cosset, F. L.; Lavillette, D.; Prieto, J.; Moreno-Otero, R.; Valenzuela-Fernandez, A.; Aldabe, R.; Lopez-Cabrera, M.; Majano, P. L. The tight junction-associated protein occludin is required for a postbinding step in hepatitis C virus entry and infection. *J. Virol.* **2009**, *83* (16), 8012–20.
(87) Carloni, G.; Crema, A.; Valli, M. B.; Ponzetto, A.; Clementi, M. HCV infection by cell-to-cell transmission: choice or necessity? *Curr. Mol. Med.* **2012**, *12* (1), 83–95.
(88) Wilson, G. K.; Brimacombe, C. L.; Rowe, I. A.; Reynolds, G. M.; Fletcher, N. F.; Stamataki, Z.; Bhogal, R. H.; Simoes, M. L.; Ashcroft, M.; Afford, S. C.; Mitry, R. R.; Dhawan, A.; Mee, C. J.; Hubscher, S. G.; Balfe, P.; McKeating, J. A. A dual role for hypoxia inducible factor-1alpha in the hepatitis C virus lifecycle and hepatoma migration. *J. Hepatol.* **2012**, *56* (4), 803–9.
(89) Daugherty, R. L.; Gottardi, C. J. Phospho-regulation of beta-catenin adhesion and signaling functions. *Physiology* **2007**, *22*, 303–9.
(90) Presser, L. D.; Haskett, A.; Waris, G. Hepatitis C virus-induced furin and thrombospondin-1 activate TGF-beta1: role of TGF-beta1 in HCV replication. *Virology* **2011**, *412* (2), 284–96.
(91) Berger, K. L.; Cooper, J. D.; Heaton, N. S.; Yoon, R.; Oakland, T. E.; Jordan, T. X.; Mateu, G.; Grakoui, A.; Randall, G. Roles for endocytic trafficking and phosphatidylinositol 4-kinase III alpha in hepatitis C virus replication. *Proc. Natl. Acad. Sci. U. S. A.* **2009**, *106* (18), 7577–82.
(92) Katsarou, K.; Lavdas, A. A.; Tsitoura, P.; Serti, E.; Markoulatos, P.; Mavromara, P.; Georgopoulou, U. Endocytosis of hepatitis C virus non-enveloped capsid-like particles induces MAPK-ERK1/2 signaling events. *Cell. Mol. Life Sci.* **2010**, *67*, 2491–506.
(93) Mankouri, J.; Griffin, S.; Harris, M. The hepatitis C virus non-structural protein NS5A alters the trafficking profile of the epidermal growth factor receptor. *Traffic* **2008**, *9* (9), 1497–509.
(94) Diao, J.; Pantua, H.; Ngu, H.; Komuves, L.; Diehl, L.; Schaefer, G.; Kapadia, S. B. Hepatitis C virus (HCV) induces epidermal growth factor receptor (EGFR) activation via CD81 binding for viral internalization and entry. *J. Virol.* **2012**, *86* (20), 10935–49.
(95) Yoon, H. Y.; Kales, S. C.; Luo, R.; Lipkowitz, S.; Randazzo, P. A. ARAP1 association with CIN85 affects epidermal growth factor receptor endocytic trafficking. *Biol. Cell* **2011**, *103* (4), 171–84.
(96) Katsarou, K.; Lavdas, A. A.; Tsitoura, P.; Serti, E.; Markoulatos, P.; Mavromara, P.; Georgopoulou, U. Endocytosis of hepatitis C virus non-enveloped capsid-like particles induces MAPK-ERK1/2 signaling events. *Cell. Mol. Life Sci.* **2010**, *67* (14), 2491–506.
(97) Diaz, A.; Ahlquist, P. Role of host reticulon proteins in rearranging membranes for positive-strand RNA virus replication. *Curr. Opin. Microbiol.* **2012**, *15* (4), 519–24.
(98) Diaz, A.; Wang, X.; Ahlquist, P. Membrane-shaping host reticulon proteins play crucial roles in viral RNA replication compartment formation and function. *Proc. Natl. Acad. Sci. U. S. A.* **2010**, *107* (37), 16291–6.
(99) Rahim, A.; Nafi-valencia, E.; Siddiqi, S.; Basha, R.; Runyon, C. C.; Siddiqi, S. A. Proteomic analysis of the very low density lipoprotein (VLDL) transport vesicles. *J Proteomics* **2012**, *75* (7), 2225–35.
(100) Coller, K. E.; Heaton, N. S.; Berger, K. L.; Cooper, J. D.; Saunders, J. L.; Randall, G. Molecular determinants and dynamics of hepatitis C virus secretion. *PLoS Pathog.* **2012**, *8* (1), e1002466.
(101) Lai, C. K.; Jeng, K. S.; Machida, K.; Lai, M. M. Association of hepatitis C virus replication complexes with microtubules and actin filaments is dependent on the interaction of NS3 and NS5A. *J. Virol.* **2008**, *82* (17), 8838–48.
(102) Randall, G.; Panis, M.; Cooper, J. D.; Tellinghuisen, T. L.; Sukhodolets, K. E.; Pfeffer, S.; Landthaler, M.; Landgraf, P.; Kan, S.; Lindenbach, B. D.; Chien, M.; Weir, D. B.; Russo, J. J.; Ju, J.; Brownstein, M. J.; Sheridan, R.; Sander, C.; Zavolan, M.; Tuschl, T.; Rice, C. M. Cellular cofactors affecting hepatitis C virus infection and replication. *Proc. Natl. Acad. Sci. U. S. A.* **2007**, *104* (31), 12884–9.
(103) Saxena, V.; Lai, C. K.; Chao, T. C.; Jeng, K. S.; Lai, M. M. Annexin A2 is involved in the formation of hepatitis C virus replication complex on the lipid raft. *J. Virol.* **2012**, *86* (8), 4139–50.
(104) Quintavalle, M.; Sambucini, S.; Summa, V.; Orsatti, L.; Talamo, F.; De Francesco, R.; Neddermann, P. Hepatitis C virus NS5A is a direct substrate of casein kinase I-alpha, a cellular kinase identified by inhibitor affinity chromatography using specific NS5A hyperphosphorylation inhibitors. *J. Biol. Chem.* **2007**, *282* (8), 5536–44.
(105) Ivanov, A. V.; Tunitskaya, V. L.; Ivanova, O. N.; Mitkevich, V. A.; Prassolov, V. S.; Makarov, A. A.; Kukhanova, M. K.; Kochetkov, S. N. Hepatitis C virus NS5A protein modulates template selection by the RNA polymerase in in vitro system. *FEBS Lett.* **2009**, *583* (2), 277–80.
(106) Park, C. Y.; Choi, S. H.; Kang, S. M.; Kang, J. I.; Ahn, B. Y.; Kim, H.; Jung, G.; Choi, K. Y.; Hwang, S. B. Nonstructural 5A protein activates beta-catenin signaling cascades: implication of hepatitis C virus-induced liver pathogenesis. *J. Hepatol.* **2009**, *51* (5), 853–64.
(107) Zhang, Z.; Harris, D.; Pandey, V. N. The FUSE binding protein is a cellular factor required for efficient replication of hepatitis C virus. *J. Virol.* **2008**, *82* (12), 5761–73.
(108) Chen, Y. J.; Chen, Y. H.; Chow, L. P.; Tsai, Y. H.; Chen, P. H.; Huang, C. Y.; Chen, W. T.; Hwang, L. H. Heat shock protein 72 is associated with the hepatitis C virus replicase complex and enhances viral RNA replication. *J. Biol. Chem.* **2010**, *285* (36), 28183–90.
(109) Choi, Y. W.; Tan, Y. J.; Lim, S. G.; Hong, W.; Goh, P. Y. Proteomic approach identifies HSP27 as an interacting partner of the hepatitis C virus NS5A protein. *Biochem. Biophys. Res. Commun.* **2004**, *318* (2), 514–9.
(110) Ahn, J.; Chung, K. S.; Kim, D. U.; Won, M.; Kim, L.; Kim, K. S.; Nam, M.; Choi, S. J.; Kim, H. C.; Yoon, M.; Chae, S. K.; Hoe, K. L. Systematic identification of hepatocellular proteins interacting with NS5A of the hepatitis C virus. *J. Biochem. Mol. Biol.* **2004**, *37* (6), 741–8.

(111) Amako, Y.; Sarkeshik, A.; Hotta, H.; Yates, J., 3rd; Siddiqui, A. Role of oxysterol binding protein in hepatitis C virus infection. *J. Virol.* **2009**, *83* (18), 9237–46.
(112) Lim, Y. S.; Tran, H. T.; Park, S. J.; Yim, S. A.; Hwang, S. B. Peptidyl-prolyl isomerase Pin1 is a cellular factor required for hepatitis C virus propagation. *J. Virol.* **2011**, *85* (17), 8777–88.
(113) Chen, Y. C.; Su, W. C.; Huang, J. Y.; Chao, T. C.; Jeng, K. S.; Machida, K.; Lai, M. M. Polo-like kinase 1 is involved in hepatitis C virus replication by hyperphosphorylating NS5A. *J. Virol.* **2010**, *84* (16), 7983–93.
(114) Waller, H.; Chatterji, U.; Gallay, P.; Parkinson, T.; Targett-Adams, P. The use of AlphaLISA technology to detect interaction between hepatitis C virus-encoded NS5A and cyclophilin A. *J. Virol. Methods* **2010**, *165* (2), 202–10.
(115) Chatterji, U.; Lim, P.; Bobardt, M. D.; Wieland, S.; Cordek, D. G.; Vuagniaux, G.; Chisari, F.; Cameron, C. E.; Targett-Adams, P.; Parkinson, T.; Gallay, P. A. HCV resistance to cyclosporin A does not correlate with a resistance of the NS5A-cyclophilin A interaction to cyclophilin inhibitors. *J. Hepatol.* **2010**, *53* (1), 50–6.
(116) Georgopoulou, U.; Tsitoura, P.; Kalamvoki, M.; Mavromara, P. The protein phosphatase 2A represents a novel cellular target for hepatitis C virus NS5A protein. *Biochimie* **2006**, *88* (6), 651–62.
(117) Helbig, K. J.; Eyre, N. S.; Yip, E.; Narayana, S.; Li, K.; Fiches, G.; McCartney, E. M.; Jangra, R. K.; Lemon, S. M.; Beard, M. R. The antiviral protein viperin inhibits hepatitis C virus replication via interaction with nonstructural protein 5A. *Hepatology* **2011**, *54* (5), 1506–17.
(118) Kumthip, K.; Chusri, P.; Jilg, N.; Zhao, L.; Fusco, D. N.; Zhao, H.; Goto, K.; Cheng, D.; Schaefer, E. A.; Zhang, L.; Pantip, C.; Thongsawat, S.; O'Brien, A.; Peng, L. F.; Maneekarn, N.; Chung, R. T.; Lin, W. Hepatitis C virus NS5A disrupts STAT1 phosphorylation and suppresses type I interferon signaling. *J. Virol.* **2012**, *86* (16), 8581–91.
(119) Inubushi, S.; Nagano-Fujii, M.; Kitayama, K.; Tanaka, M.; An, C.; Yokozaki, H.; Yamamura, H.; Nuriya, H.; Kohara, M.; Sada, K.; Hotta, H. Hepatitis C virus NS5A protein interacts with and negatively regulates the non-receptor protein tyrosine kinase Syk. *J. Gen. Virol.* **2008**, *89* (Pt 5), 1231–42.

Biochemical and Biophysical Research Communications 438 (2013) 230–235

Contents lists available at ScienceDirect

Biochemical and Biophysical Research Communications

journal homepage: www.elsevier.com/locate/ybbrc

Inhibition of microRNA122 decreases SREBP1 expression by modulating suppressor of cytokine signaling 3 expression

Chikako Shibata [a], Takahiro Kishikawa [a], Motoyuki Otsuka [a,b,*], Motoko Ohno [a], Takeshi Yoshikawa [a], Akemi Takata [a], Haruhiko Yoshida [a], Kazuhiko Koike [a]

[a] Department of Gastroenterology, Graduate School of Medicine, The University of Tokyo, Tokyo 113-8655, Japan
[b] Japan Science and Technology Agency, PRESTO, Kawaguchi, Saitama 332-0012, Japan

ARTICLE INFO

Article history:
Received 13 July 2013
Available online 24 July 2013

Keywords:
microRNA
Liver
SOCS3
SREBP
Expression regulation

ABSTRACT

While inhibition of microRNA122 (miR122) function *in vivo* results in reduced serum cholesterol and fatty acid levels, the molecular mechanisms underlying the link between miR122 function and lipid metabolism remains unclear. Because the expression of SREBP1, a central transcription factor involved in lipid metabolism, is known to be increased by suppressor of cytokine signaling 3 (SOCS3) expression, and because we previously found that SOCS3 expression is regulated by miR122, in this study, we examined the correlation between miR122 status and the expression levels of SOCS3 and SREBP1. SREBP1 expression decreased when SOCS3 expression was reduced by miR122 silencing *in vitro*. Conversely, SREBP1 expression in miR122-silenced cells was restored by enforced expression of SOCS3. Such correlations were observed in human liver tissues with different miR122 expression levels. These signaling links may explain one of the molecular mechanisms linking inhibition of miR122 function or decreased expression of miR122 to decreased fatty acid and cholesterol levels, in the inhibition of miR122 function, or in pathological status in chronic liver diseases.

1. Introduction

MiRNA122 (miR122) is the most abundant and tissue-specific miRNA in the liver [1], and inhibition of miR122 *in vivo* was shown to greatly reduce serum cholesterol and fatty acid levels [2–6]. Recently, miravirsen, a locked nucleic acid-modified DNA phosphorothioate antisense oligonucleotide against miR122, was introduced practically to reduce hepatitis C virus (HCV) RNA levels in patients with HCV infection [7]. Although the primary purpose of the trial was to inhibit HCV replication, lipid levels were also found to decrease [7]. Despite consistent results concerning miR-122-mediated lipid metabolism, the underlying molecular mechanisms remain unclear, and although the expression levels of genes associated with lipid metabolism were affected by miR-122 inhibition, these genes were not direct targets of miR122, as judged by sequence similarities.

Members of the family of sterol regulatory element-binding proteins (SREBPs) are critical regulators of cholesterol and lipid homeostasis. The SBEBP family belongs to the basic helix–loop–helix–leucine zipper (bHLH-zipper) family of transcription factors and comprises SREBP-1a, SREBP-1c, and SREBP-2. The SREBF-1 gene on chromosome 17p11.2 encodes SREBP-1a and SREBP-1c, which are generated as alternatively spliced variants. Increased SREBP activity causes cholesterol and fatty acid accumulation by activating the expression of more than 30 genes dedicated to the synthesis and uptake of cholesterol, fatty acids, triglycerides, and phospholipids, as well as the NADPH cofactor required for synthesis of these molecules [8], which increases lipid levels.

The promoter activities of SREBP1 are potently inhibited by activated STAT3 [9]. In addition, STAT3-mediated inhibition of SREBP1 expression was shown to be antagonized by co-expression of the SOCS3 protein [9]. Conversely, SOCS3 inhibition in the liver in obese mice subjected to antisense treatment was reported to completely normalize the increased expression of SREBP1, leading to dramatic amelioration of hyperlipidemia. These results indicate the importance of SOCS3 in regulating SREBP expression and subsequent lipid metabolism [9].

We recently reported that silencing miR122 in hepatocytes leads to decreased SOCS3 expression accompanied by hypermethylation of the SOCS3 promoter in a Dnmt1-independent manner [10]. In this study, we first assessed the correlated expression levels of SREBP1 in miR122-silenced and miR122 precursor-overexpressing cells. In addition, SREBP1 was recovered by enforced expression or inhibition of SOCS3 in miR122-modulated cells. We next confirmed the correlations among miR122, SOCS3, and SREBP

* Corresponding author. Address: Department of Gastroenterology, Graduate School of Medicine, The University of Tokyo, 5-3-1 Hongo, Bunkyo-ku, Tokyo 113-8655, Japan. Fax: +81 3 3814 0021.
E-mail address: otsukamo-tky@umin.ac.jp (M. Otsuka).

0006-291X/$ - see front matter © 2013 Elsevier Inc. All rights reserved.
http://dx.doi.org/10.1016/j.bbrc.2013.07.064

expression levels in human liver tissues in various pathological states with different miR122 expression levels [11]. Based on these analyses, we infer a molecular link between miR122 and lipid metabolism in miR122 inhibition and various liver pathological states.

2. Methods

2.1. Cells

The Huh7 and Hep3B human hepatocellular carcinoma cell lines were obtained from the Japanese Collection of Research Bioresources (JCRB, Osaka, Japan). Cells were maintained in Dulbecco's modified Eagle's medium (DMEM) supplemented with 10% fetal bovine serum.

2.2. Plasmids, viral production, and transduction

A miR122 precursor-expressing plasmid with a puromycin resistance gene (pCDH-miR122 with puro) and an H1 promoter-driven antisense miR122 stem–loop–stem RNA-expressing plasmid (pmiRZIP122 with puro) were constructed as described previously [10]. For double stable Hep3B cells with miR122 precursor and SOCS3 shRNA expression, a miR122 precursor with hygromycin resistance gene (pCDH-miR122 with hygro) was constructed by replacement of the puromycin resistance gene with a hygromycin resistant gene using the infusion method (Clontech, Mountain View, CA). SOCS3 shRNA-expressing lentiviral particles were purchased from Santa Cruz Biotechnology (Dallas, TX). An HA-SOCS3-expressing lentiviral construct with a neomycin resistance gene was constructed as described previously [10]. A pCDH control vector (System Biosciences, Mountain View, CA) was used as a negative control. Lentiviral particles, produced using pPACKH1 lentivector packaging plasmid mix (System Biosciences) according to the manufacturer's recommendations, were used as a negative control. Cells were transduced with lentiviruses using polybrene (EMD Millipore, Billerica, MA) and were then selected using puromycin.

2.3. Reporter plasmids, transient transfections, and luciferase assays

The reporter plasmids used for analysis of miR122 function were constructed as described previously [12]. Plasmid transfection was performed using FuGene6 Transfection Reagent (Boehringer Mannheim, Mannheim, Germany) according to the manufacturer's instructions. pGL4-TK, a control plasmid containing *Renilla reniformis* (sea pansy) luciferase under the control of the herpes simplex virus thymidine kinase promoter (Promega, Madison, WI), was used to determine transfection efficiency. Relative luciferase values were calculated by normalizing firefly luciferase activity values to sea pansy luciferase activity values to account for changes in transfection efficiency. Luciferase activity was measured using a Dual Luciferase Reporter Assay System (Promega) with a Lumat LB9507 luminometer (EG&G Berthold, Bad Wildbad, Germany).

2.4. Northern blotting of miRNAs

Northern blotting of miRNAs was performed as described previously [23]. Briefly, total RNA was extracted using TRIzol Reagent (Invitrogen, Carlsbad, CA). Ten micrograms of RNA was resolved in denaturing 15% polyacrylamide gels containing 7 M urea in 1× TBE and then transferred to a Hybond N+ membrane (GE Healthcare, Milwaukee, WI) in 0.25× TBE. Membranes were UV-cross-linked and prehybridized in hybridization buffer. Hybridization was performed overnight at 42 °C in ULTRAhyb-Oligo Buffer (Ambion, Austin, TX) containing a biotinylated probe specific for miR122 (tgg agt gtg aca atg gtg ttt g), antisense miR122 (caa aca cca ttg tca cac tcc a), or U6 (cac gaa ttt gcg tgt cat cct t), which had previously been heated at 95 °C for 2 min. Membranes were washed at 42 °C in 2× SSC containing 0.1% SDS, and the bound probe was visualized using a BrightStar BioDetect Kit (Ambion). A pre-stained RNA size marker for small RNA (BioDynamics Laboratory, Tokyo, Japan) was used to estimate band sizes. Blots were stripped by boiling in a solution containing 0.1% SDS and 5 mM EDTA for 10 min prior to rehybridization.

2.5. Western blot analysis and antibodies

Western blotting was performed as described previously [12]. Anti-SREBP was purchased from Santa Cruz Biotechnology. Anti-β-actin was acquired from Sigma–Aldrich (St. Louis, MO). An anti-HA antibody was obtained from Roche Applied Science (Penzberg, Germany). Other antibodies were purchased from Cell Signaling Technology (Danvers, MA).

2.6. Immunohistochemistry

Tissue arrays containing liver tissues (LV1504) were purchased from US Biomax (Rockville, MD). Immunohistochemistry was performed as described previously [23]. Briefly, after deparaffinization of the slides, endogenous peroxidase activity was blocked with 3% hydrogen peroxide buffer. Antigen retrieval was achieved by incubating the slides at 89 °C in 10 mM sodium citrate buffer (pH 6.0) for 30 min. To minimize nonspecific background staining, slides were blocked in 5% normal goat serum (Dako, Glostrup, Denmark). Tissues were labeled overnight at 4 °C with primary antibodies raised against SOCS3 or SREBP1. Slides were then incubated with an anti-mouse horseradish peroxidase-conjugated secondary antibody (Nichirei Bioscience, Tokyo, Japan) for 1 h. Bound antibody was visualized by incubation in 3,3′-diaminobenzidine (Nichirei Bioscience) for 5 min. The slides were counterstained with hematoxylin, dehydrated with ethanol, and mounted using Clarion mounting medium (Biomeda, Foster City, CA).

2.7. In situ hybridization to assess miR122

Locked nucleic acid (LNA)-scramble (negative control), LNA-anti-U6 (positive control), and LNA-anti-miR122 probes were obtained from EXIQON (Vedbæk, Denmark). The expression of miR122 in liver tissues was examined by *in situ* hybridization as described previously [12]. Briefly, after deparaffinization, tissue sections were treated with 10 μg/ml proteinase K for 5 min at 37 °C, refixed with 4% paraformaldehyde, and acetylated with 0.25% anhydrous acetic acid in 0.1 M Tris–HCl buffer (pH 8.0). Following prehybridization for 30 min at 48 °C, hybridization was performed overnight with each LNA probe (20 nM) in hybridization buffer (5× SSC buffer, 50% formamide, 500 μg/ml tRNA, 50 μg/ml Cot-1 DNA). After the completion of hybridization, the sections were washed with 0.1× SSC buffer for 10 min at 52 °C three times and blocked with DIG blocking buffer (Roche Diagnostics, Basel, Switzerland) for 30 min. Sections were then probed with anti-DIG (1:500; Roche Diagnostics) for 1 h at room temperature. Detection was performed by incubation in NBT/BCIP buffer (Promega) overnight. Nuclei were stained with Nuclear Fast Red (Sigma–Aldrich).

2.8. Histological scoring

Tissue staining was scored as described previously [23]. Briefly, staining intensity was semiquantitatively categorized into the

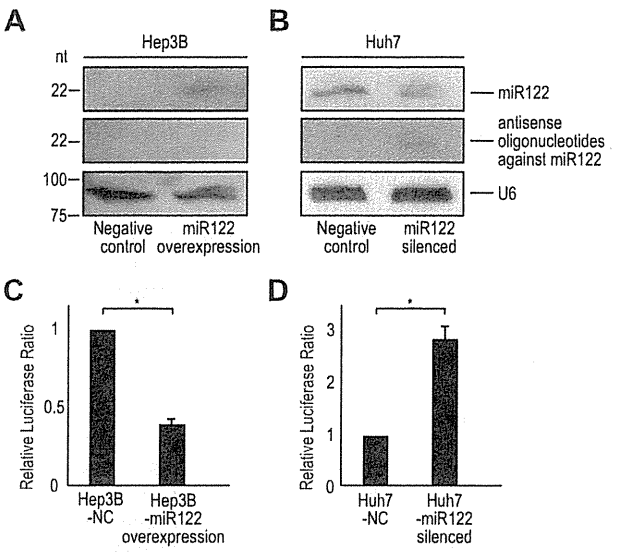

Fig. 1. Establishing of miR122-overexpressing and miR122-silenced cell lines. A, B, Northern blotting against miR122 and miR122 antisense oligonucleotides in Hep3B cells (A) and Huh7 cells (B). U6 levels were used as a loading control. Representative images from three independent experiments are shown. C, D, Luciferase expression from the reporter construct containing two tandem miR122 responsive elements in its 3'UTR, which are targeted by miR122, were examined. The suppressive effects of stably miR122 precursor-overexpressing Hep3B cells (C) and silencing effects on endogenous miR122 function in stably miR122 antisense-expressing Huh7 cells (D) are shown. Test values were normalized to those obtained from the cells transduced with a miRNA precursor-non-expressing negative control, which were set to 1 (nc). Data represent the mean ± standard deviations (SD) of three independent experiments.

following four categories by two independent investigators: –, no staining; +, weak staining; ++, moderate staining; and +++, intense staining. The color scale reflects staining intensity from green (no staining) to pink (intense staining).

2.9. Statistical analysis

Statistically significant differences between groups were determined using Student's *t*-test. *P*-values less than 0.05 were considered statistically significant.

3. Results

3.1. Establishment of miR122-overexpressing and -silenced cell lines

To determine the function of miR122, we modulated miR122 expression levels and function in liver cell lines by overexpressing an miR122 precursor construct or antisense sequences, respectively, against miR122, as previously reported [10,12]. Because Hep3B cells have relatively low miR122 expression and Huh7 cells have relatively high miR122 expression [13], we constructed miR122-overexpressing Hep3B cells and miR122-silenced Huh7 cells to examine the effects of modulating miR122. Overexpression of the miR122 precursor construct in Hep3B cells was confirmed by Northern blotting against miR122 sequences (Fig. 1A). Expression of the antisense construct against miR122 in Huh7 cells in Northern blotting appeared to be lower when using a probe to detect antisense miR122 (Fig. 1B). In these cells, miR122 levels were also lower, although miR122 was highly expressed in control Huh7 cells (Fig. 1B), suggesting that introduction of the antisense construct against miR122 may result not only in sequestration of endogenous miR122 by binding but also degradation of endogenous miR122 after formation of double-stranded RNA composed of sense and antisense miR122.

Next, we confirmed the changes in miR122 function using a luciferase reporter targeted by miR122. As predicted, in miR122-overexpressing Hep3B cells, luciferase activity decreased by more than half due to the ectopic miR122 expression (Fig. 1C). In contrast, in miR122-silenced Huh7 cells, luciferase activity increased about three times compared to control cells (Fig. 1D). These results suggest that modulation of miR122 by overexpressing exogenous constructs targeting miR122 was efficient.

3.2. SOCS3 and SREBP1 expression is decreased by miR122 silencing

Because we previously reported that miR122 silencing increased methylation in the promoter region of the SOCS3 gene and decreased its expression [10], we confirmed the expression levels of SOCS3 in miR122-overexpressing Hep3B cells and miR122-silenced Huh7 cells. Consistent with previous reports [10], SOCS3 expression increased and was downregulated in miR122-overexpressing Hep3B cells and miR122-silenced Huh7 cells, respectively (Fig. 2A and B). SOCS3 is a potent inhibitor of STAT3 activation [14]. Thus, we examined the phosphorylation status of STAT3. While total STAT3 expression levels remained unchanged, STAT3 phosphorylation decreased in miR122-overexpressing Hep3B cells and was higher in miR122-silenced Huh7 cells (Fig. 2A and B), suggesting that miR122 overexpression results in decreased STAT3 activation and that miR122 silencing has the opposite effect. Because a previous report revealed that STAT3 inhibits the promoter activity of SREBP1, a key regulator of fatty acid synthesis in the liver, we next examined the

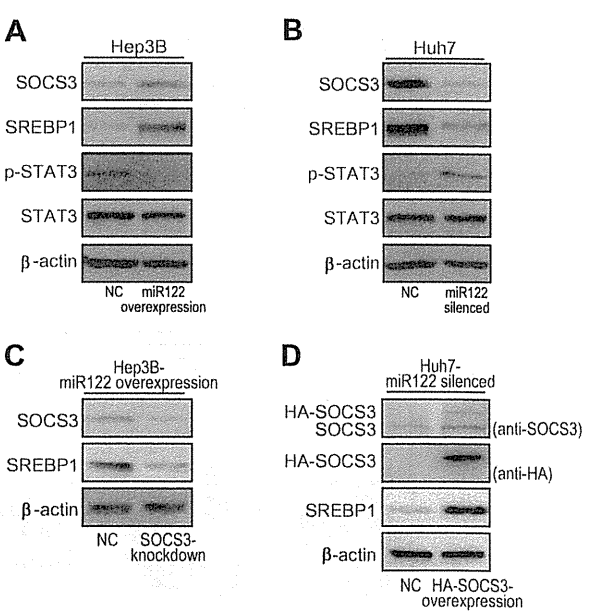

Fig. 2. SREBP1 expression is regulated by SOCS3. (A and B) SOCS3, SREBP1, and STAT3 protein expression levels and phosphorylation levels of STAT3 were determined by western blotting. Representative results from three independent experiments using Hep3B cells (A) and miR122-silenced Huh7 cells (B) are shown. (C) The effects of SOCS3 knockdown on SREBP expression in miR122 overexpressing Hep3B cell were stably transduced with SOCS3 shRNA. Representative results from three independent experiments are shown. (D) The effects of SOCS3 overexpression on SREBP expression in miR122-silenced Huh7 cells. Indicated protein expression levels were determined after miR122-silenced Huh7 cells were stably transduced with HA-SOCS3 expressing lentiviruses. HA-SOCS3 was visualized using anti-SOCS3 (the upper panel) and anti-HA (the second panel). Representative results from three independent experiments are shown.

expression levels of SREBP1 in miR122-modulated cells. The expression of SREBP1 was found to increase in miR122-overexpressing Hep3B cells and decrease in miR122-silenced Huh7 cells (Fig. 2A and B).

To confirm the role of OSCS3 in SREBP1 expression, we determined the effects of knockdown of SOCS3 expression in miR122-overexpresing Hep3B cells and enforced the expression of SOCS3 in miR122-silenced Huh7 cells (Fig. 2C and D). Knockdown of SOCS3 in miR122-overexpressing Hep3B cells reduced SREBP1 expression and enforced the expression of SOCS3 in miR122-silenced Huh7 cells increased SREBP1 expression (Fig. 2C and D). These results suggest that miR122 upregulates SOCS3 expression, resulting in the inhibition of STAT3 activation and subsequent upregulation of SREBP1 expression, and that inhibition of miR122 has the opposite effect.

3.3. Correlation of miR122, SOCS3, and SREBP1 expression levels in human liver tissues

To confirm the above results in human clinical liver tissues, we examined 50 human liver tissues for the expression levels of miR122, SOCS3, and SREBP1 by *in situ* hybridization and immunohistochemistry (Fig. 3A and B). The expression levels of miR122 varied in liver tissues under various conditions (Fig. 3). When the expression levels of miR122 were reduced, the expression levels of SOCS3 and SREBP1 also decreased in more than 70% of cases (Fig. 3C). As previously reported [11,15], the expression levels of miR122 tended to decrease in liver cirrhosis, and SOCS3 and SREBP1 levels typically also decreased under such pathological conditions (Fig. 3C and Supplementary Table 1). These results may explain, at least in part, the decreased fatty acid and cholesterol synthesis observed clinically in the cirrhotic liver.

4. Discussion

In this study, we demonstrated that silencing miR122 function in liver cells resulted in decreased expression of SOCS3, and subsequently, decreased the expression of SREBP1. Because SREBP1 plays a key role in regulating fatty acid and cholesterol synthesis, reduced expression of miR122, which is frequently observed clinically in various chronic liver diseases [11,15], may be a cause of the decreased fatty acid and cholesterol synthesis in such pathological

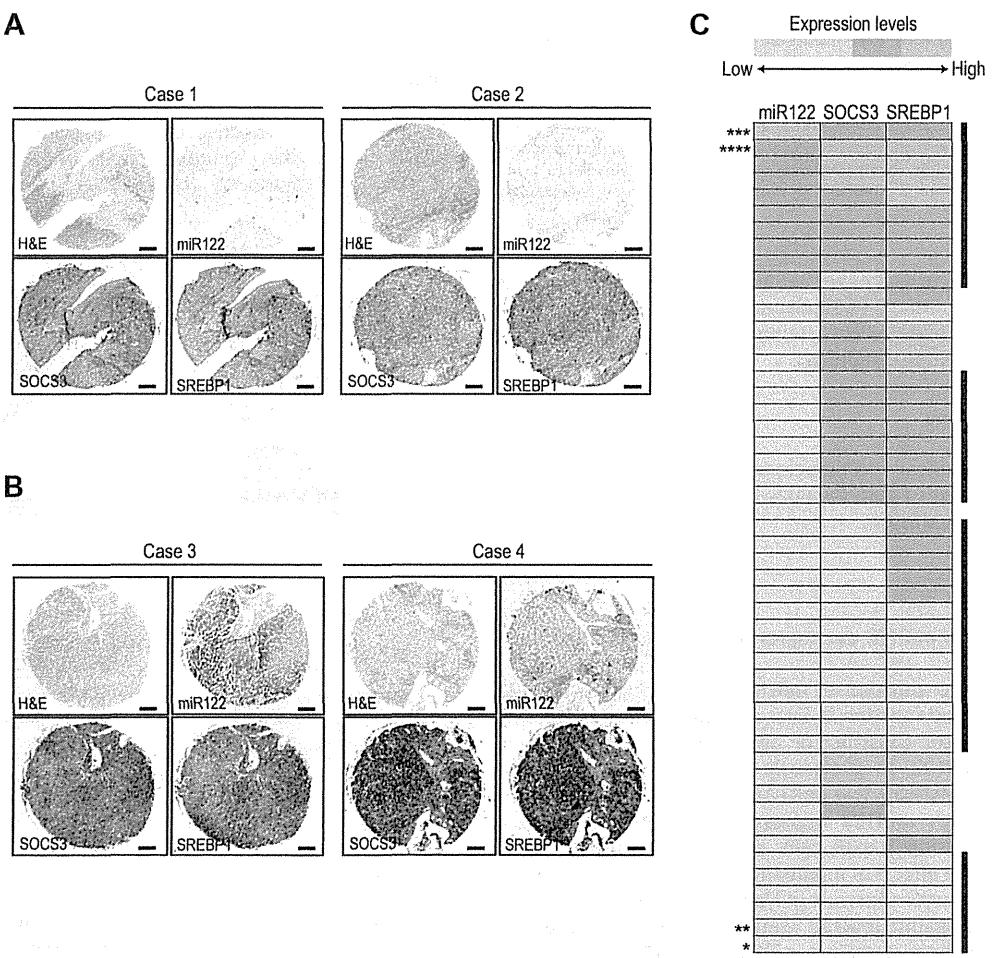

Fig. 3. Correlation of miR122, SOCS3, and SREBP expression levels in human liver tissues. (A and B), Representative liver tissues from four cases with correlated low (A) and high (B) expression levels of miR122, SOCS3, and SREBP. MiR122 was visualized by *in situ* hybridization (blue) and nuclei were stained with Nuclear Red (pink). SOCS3 and SREBP1 were stained by immunohistochemistry (brown). Bars, 500 μm. Hematoxylin and eosin (H&E)-stained tissues from each case are also shown as references. (C) Summarized expression levels of miR122, SOCS3, and SREBP1 in liver tissues from 50 cases. The color reflects the expression level of each parameter examined. Green denotes the lowest expression level and pink the highest, as the color scale bar at the top indicates. In 37 cases (indicated by black bars to the right), the differences between the expression scores of the three parameters are within one point on the color scale. *, Case 1 (A); **, Case 2 (A); ***, Case 3 (B); ****, Case 4 (B). (For interpretation of the references to color in this figure legend, the reader is referred to the web version of this article.)

states. In addition, silencing miR122 function decreases cholesterol and fatty acid levels [2–7]. While miR122 does not directly target known fatty acid-related molecules based on sequence similarities, the results of this study may explain the molecular mechanism linking miR122 silencing to decreased fatty acid and cholesterol levels.

We previously reported that silencing miR122 leads to decreased SOCS3 expression levels and increased SOCS3 promoter methylation in a Dnmt1-independent manner [10]. Such correlations in human clinical tissues were confirmed in most cases in this study. However, some cases did not show such a correlation, perhaps because while SOCS3 expression is mainly regulated by methylation of its promoter [16,17], such modifications are probably not mediated solely by miR122. Nonetheless, the decrease in SOCS3 expression that frequently accompanies decreased miR122 expression in chronic liver pathological states suggests that the SOCS3 expression in hepatocytes is largely regulated by miR122 expression or function.

The expression of SREBP1 is negatively regulated by activated STAT3, which inhibits SREBP1 promoter activities [9]. Decreased SREBP1 expression caused by increased STAT3 activity, which was itself due to decreased SOCS3 expression, was observed in miR122-silenced Huh7 cells and in liver tissues with decreased miR122 expression. Because miR122 expression levels tend to decrease as the pathological status of the liver progresses from chronic hepatitis to liver cirrhosis [11,15], observing a decreased synthesis of fatty acid and cholesterol in progressed chronic liver diseases such as liver cirrhosis may be reasonable.

One complex liver pathological situation from this point of view is obese subjects with fatty liver and insulin resistance. In these subjects, persistently elevated cytokine levels may have downregulated STAT3-mediated signaling by increasing SOCS3 protein levels in the liver [18]. Increased SOCS3 protein levels may in turn increase fatty acid synthesis by upregulating SREBP1 expression, presumably through suppression of STAT3 activation [18]. Overproduction of fatty acids and lipotoxicity result in further insulin resistance [19]. However, as these pathological conditions persist, liver cirrhosis gradually becomes apparent and fatty acid synthesis decreases. At this stage, miR122 expression in the liver becomes low [11]. Thus, in these cases, the effects of decreased miR122 expression may become apparent for the first time at the later stages of disease progression, which may be one of the reasons why not all cases showed an exact correlation between miR122 expression and SREBP levels in clinical samples.

Recently, miravirsen, an anti-miR122 oligonucleotide, was successfully applied as a novel therapeutic against HCV [7]. Although the main purpose of applying antisense miR122 *in vivo* is at present to inhibit HCV replication, decreased fatty acid and cholesterol levels were also reported [7]. In several *in vivo* experiments, antisense miR122 reduced serum lipid levels [3–5]. In addition, mice with a miR122 gene deletion in the liver showed reduced fatty acid and cholesterol levels [2,20], despite SREBP1 not being a direct target of miR122. The molecular pathway reported here may explain the reduced lipid levels observed in miR122 inhibition or gene deletion. Moreover, from these results, inhibiting miR122 may be a promising approach to controlling serum lipid levels, although the long-term inhibition of miR122 must be confirmed to be safe with no unfavorable consequences because miRNAs have pleiotropic effects [21,22].

Author contributions

C.S. and M.O. planned the research and wrote the paper. C.S., T.K., M.O., M.O., T.Y., and A.Y. performed the majority of the experiments. H.Y. supported several experiments. K.K. supervised the entire project.

Acknowledgments

This work was supported by Grants-in-Aid from the Ministry of Education, Culture, Sports, Science and Technology, Japan (#25293076 and #24390183) (to M.O. and K.K.), by Health Sciences Research Grants of The Ministry of Health, Labour and Welfare of Japan (to K.K.), and a Grant from the Japanese Society of Gastroenterology (to M.O.).

Appendix A. Supplementary data

Supplementary data associated with this article can be found, in the online version, at http://dx.doi.org/10.1016/j.bbrc.2013.07.064.

References

[1] P. Landgraf, M. Rusu, R. Sheridan, A. Sewer, N. Iovino, A. Aravin, S. Pfeffer, A. Rice, A. Kamphorst, M. Landthaler, C. Lin, N. Socci, L. Hermida, V. Fulci, S. Chiaretti, R. Foà, J. Schliwka, U. Fuchs, A. Novosel, R. Müller, B. Schermer, U. Bissels, J. Inman, Q. Phan, M. Chien, D. Weir, R. Choksi, G. De Vita, D. Frezzetti, H. Trompeter, V. Hornung, G. Teng, G. Hartmann, M. Palkovits, R. Di Lauro, P. Wernet, G. Macino, C. Rogler, J. Nagle, J. Ju, F. Papavasiliou, T. Benzing, P. Lichter, W. Tam, M. Brownstein, A. Bosio, A. Borkhardt, J. Russo, C. Sander, M. Zavolan, T. Tuschl, A mammalian microRNA expression atlas based on small RNA library sequencing, Cell 129 (2007) 1401–1414.

[2] S.H. Hsu, B. Wang, J. Kota, J. Yu, S. Costinean, H. Kutay, L. Yu, S. Bai, K. La Perle, R.R. Chivukula, H. Mao, M. Wei, K.R. Clark, J.R. Mendell, M.A. Caligiuri, S.T. Jacob, J.T. Mendell, K. Ghoshal, Essential metabolic, anti-inflammatory, and anti-tumorigenic functions of miR-122 in liver, J. Clin. Invest. 122 (2012) 2871–2883.

[3] R.E. Lanford, E.S. Hildebrandt-Eriksen, A. Petri, R. Persson, M. Lindow, M.E. Munk, S. Kauppinen, H. Ørum, Therapeutic silencing of microRNA-122 in primates with chronic hepatitis C virus infection, Science 327 (2010) 198–201.

[4] J. Elmén, M. Lindow, S. Schütz, M. Lawrence, A. Petri, S. Obad, M. Lindholm, M. Hedtjärn, H.F. Hansen, U. Berger, S. Gullans, P. Kearney, P. Sarnow, E.M. Straarup, S. Kauppinen, LNA-mediated microRNA silencing in non-human primates, Nature 452 (2008) 896–899.

[5] C. Esau, S. Davis, S.F. Murray, X.X. Yu, S.K. Pandey, M. Pear, L. Watts, S.L. Booten, M. Graham, R. McKay, A. Subramaniam, S. Propp, B.A. Lollo, S. Freier, C.F. Bennett, S. Bhanot, B.P. Monia, MiR-122 regulation of lipid metabolism revealed by *in vivo* antisense targeting, Cell Metab. 3 (2006) 87–98.

[6] J. Krützfeldt, N. Rajewsky, R. Braich, K. Rajeev, T. Tuschl, M. Manoharan, M. Stoffel, Silencing of microRNAs *in vivo* with 'antagomirs', Nature 438 (2005) 685–689.

[7] H.L. Janssen, H.W. Reesink, E.J. Lawitz, S. Zeuzem, M. Rodriguez-Torres, K. Patel, A.J. van der Meer, A.K. Patick, A. Chen, Y. Zhou, R. Persson, B.D. King, S. Kauppinen, A.A. Levin, M.R. Hodges, Treatment of HCV Infection by targeting MicroRNA, N. Engl. J. Med. 368 (2013) 1685–1694.

[8] J.D. Horton, Sterol regulatory element-binding proteins: transcriptional activators of lipid synthesis, Biochem. Soc. Trans. 30 (2002) 1091–1095.

[9] K. Ueki, T. Kondo, Y.H. Tseng, C.R. Kahn, Central role of suppressors of cytokine signaling proteins in hepatic steatosis, insulin resistance, and the metabolic syndrome in the mouse, Proc Natl Acad Sci U S A 101 (2004) 10422–10427.

[10] T. Yoshikawa, A. Takata, M. Otsuka, T. Kishikawa, K. Kojima, H. Yoshida, K. Koike, Silencing of microRNA-122 enhances interferon-[agr] signaling in the liver through regulating SOCS3 promoter methylation, Sci. Rep. 2 (2012).

[11] R.T. Marquez, S. Bandyopadhyay, E.B. Wendlandt, K. Keck, B.A. Hoffer, M.S. Icardi, R.N. Christensen, W.N. Schmidt, A.P. McCaffrey, Correlation between microRNA expression levels and clinical parameters associated with chronic hepatitis C viral infection in humans, Lab Invest. 90 (2010) 1727–1736.

[12] K. Kojima, A. Takata, C. Vadnais, M. Otsuka, T. Yoshikawa, M. Akanuma, Y. Kondo, Y.J. Kang, T. Kishikawa, N. Kato, Z. Xie, W.J. Zhang, H. Yoshida, M. Omata, A. Nepveu, K. Koike, MicroRNA122 is a key regulator of α-fetoprotein expression and influences the aggressiveness of hepatocellular carcinoma, Nat. Commun. 2 (2011) 338.

[13] S. Bai, M. Nasser, B. Wang, S. Hsu, J. Datta, H. Kutay, A. Yadav, G. Nuovo, P. Kumar, K. Ghoshal, MicroRNA-122 inhibits tumorigenic properties of hepatocellular carcinoma cells and sensitizes these cells to sorafenib, J. Biol. Chem. 284 (2009) 32015–32027.

[14] A. Yoshimura, The CIS family: negative regulators of JAK-STAT signaling, Cytokine Growth Factor Rev. 9 (1998) 197–204.

[15] K. Morita, A. Taketomi, K. Shirabe, K. Umeda, H. Kayashima, M. Ninomiya, H. Uchiyama, Y. Soejima, Y. Maehara, Clinical significance and potential of hepatic microRNA-122 expression in hepatitis C, Liver Int. 31 (2011) 474–484.

[16] B. He, L. You, K. Uematsu, K. Zang, Z. Xu, A.Y. Lee, J.F. Costello, F. McCormick, D.M. Jablons, SOCS-3 is frequently silenced by hypermethylation and suppresses cell growth in human lung cancer, Proc. Natl. Acad. Sci. USA 100 (2003) 14133–14138.

[17] Y. Niwa, H. Kanda, Y. Shikauchi, A. Saiura, K. Matsubara, T. Kitagawa, J. Yamamoto, T. Kubo, H. Yoshikawa, Methylation silencing of SOCS-3 promotes

cell growth and migration by enhancing JAK/STAT and FAK signalings in human hepatocellular carcinoma, Oncogene 24 (2005) 6406–6417.
[18] H. Tilg, The role of cytokines in non-alcoholic fatty liver disease, Dig. Dis. 28 (2010) 179–185.
[19] V.T. Samuel, K.F. Petersen, G.I. Shulman, Lipid-induced insulin resistance: unravelling the mechanism, Lancet 375 (2010) 2267–2277.
[20] W.C. Tsai, S.D. Hsu, C.S. Hsu, T.C. Lai, S.J. Chen, R. Shen, Y. Huang, H.C. Chen, C.H. Lee, T.F. Tsai, M.T. Hsu, J.C. Wu, H.D. Huang, M.S. Shiao, M. Hsiao, A.P. Tsou, MicroRNA-122 plays a critical role in liver homeostasis and hepatocarcinogenesis, J. Clin. Invest. 122 (2012) 2884–2897.
[21] G. Szabo, P. Sarnow, S. Bala, MicroRNA silencing and the development of novel therapies for liver disease, J. Hepatol. 57 (2012) 462–466.
[22] S.P. Nana-Sinkam, C.M. Croce, Clinical applications for microRNAs in cancer, Clin. Pharmacol. Ther. 93 (2013) 98–104.
[23] A. Takata, M. Otsuka, T. Yoshikawa, T. Kishikawa, Y. Hikiba, S. Obi, T. Goto, Y.J. Kang, S. Maeda, H. Yoshida, M. Omata, H. Asahara, K. Koike, MicroRNA-140 acts as a liver tumor suppressor by controlling NF-κB activity by directly targeting DNA methyltransferase 1 (Dnmt1) expression, Hepatology 57 (2013) 162–170.

J Gastroenterol
DOI 10.1007/s00535-013-0843-9

ORIGINAL ARTICLE—LIVER, PANCREAS, AND BILIARY TRACT

Acute liver disease in Japan: a nationwide analysis of the Japanese Diagnosis Procedure Combination database

Masaya Sato · Ryosuke Tateishi · Hideo Yasunaga · Hiromasa Horiguchi · Haruhiko Yoshida · Shinya Matsuda · Kiyohide Fushimi · Kazuhiko Koike

Received: 30 November 2012 / Accepted: 23 May 2013

Abstract
Background Accurate data on the incidence of acute liver disease (ALD) is lacking in most countries. We investigated the incidence of ALD-related admission in Japan using a large sample in a nationwide Japanese database.
Methods Data from the Diagnosis Procedure Combination database were analyzed for 1 July to 31 December 2007–2010. Patient characteristics, in-hospital mortality, and clinical practices, including drugs and procedures during hospitalization, were analyzed.
Results We identified 10509 patients with ALD from a total of 11.61 million inpatients in the database. The median age was 53 years and 54.7 % were male. The annual incidence of ALD-related hospital admission was estimated to be 131.1 cases/1 million people. The overall mortality rate was 5.9 % (622 cases). The infant (0–3 years), child (4–18 years), and adult in-hospital mortality rates were 2.7 % (7/261), 1.0 % (5/494), and 6.3 % (610/9754), respectively. The infant and child mortality rates were significantly lower than the adult mortality rate (Chi square test: $P = 0.03$ and $P < 0.001$, respectively). Hepatitis A virus- and hepatitis C virus-induced ALD had favorable outcomes, with in-hospital mortality rates of approximately 2 %. Plasma exchange and continuous hemodiafiltration were performed in 5.3 % (556 cases) and 3.4 % (360 cases) of all ALD cases, respectively.
Conclusions In-hospital mortality of ALD in Japan was acceptably low, and was affected by the etiology and patient background characteristics. The present study adds important information on the incidence and prognosis of ALD in Japan. Improvement of public health surveillance systems is necessary for population-based patient monitoring.

Keywords Acute hepatitis · Diagnosis Procedure Combination · Nationwide database · In-hospital mortality · Clinical practices

Abbreviations

AIH	Autoimmune hepatitis
ALD	Acute liver disease
ALF	Acute liver failure
A/AoCLF	Acute or acute-on-chronic liver failure
CHDF	Continuous hemodiafiltration
DPC	Diagnosis Procedure Combination
FH	Fulminant hepatitis
HAV	Hepatitis A virus
HBV	Hepatitis B virus
HCV	Hepatitis C virus
HEV	Hepatitis E virus
ICD-10	International classification of diseases and related health problems, tenth revision

M. Sato · R. Tateishi (✉) · H. Yoshida · K. Koike
Department of Gastroenterology, Graduate School of Medicine, The University of Tokyo, 7-3-1 Hongo, Bunkyo-ku, Tokyo 113-8655, Japan
e-mail: tateishi-tky@umin.ac.jp

H. Yasunaga · H. Horiguchi
Department of Health Management and Policy, Graduate School of Medicine, The University of Tokyo, Tokyo, Japan

S. Matsuda
Department of Preventive Medicine and Community Health, University of Occupational and Environmental Health, Fukuoka, Japan

K. Fushimi
Department of Health Policy and Informatics, Graduate School of Medicine, Tokyo Medical and Dental University, Tokyo, Japan

Published online: 20 June 2013

Introduction

Acute liver disease (ALD) is characterized by acute inflammation with varying degrees of necrosis and collapse of the hepatic architectural framework. ALD is generally a transient self-limiting disease regardless of the etiology. However, the severity of the disease is variable, and some patients progress to a fatal form, acute liver failure (ALF). ALF is a serious but rare clinical syndrome marked by sudden loss of hepatic function in a person with no prior history of liver disease. Clinically, the syndrome manifests itself as a severe impairment of liver function with hepatocellular necrosis, leading to hepatic encephalopathy, systemic inflammation, and multiorgan failure [1, 2].

In Japan, the definition and classification of fulminant hepatitis (FH), which was the representative disease entity associated with ALF, were originally established at the Inuyama Symposium in 1981 [3]. However, because of the differences in the demographic and clinical features of ALF between Japan and Europe or the United States, the diagnostic criteria for FH in Japan differed from those for ALF in Europe and the United States [4, 5]. Therefore, the diagnostic criteria for FH in Japan needed to be revised to correspond to those for ALF in Europe and the United States, and the Intractable Hepato-Biliary Disease Study Group of Japan recently determined the diagnostic criteria for ALF [6, 7].

Since the wide variety of symptoms in ALD makes it challenging to establish surveillance systems, accurate data on the incidence of ALD is lacking in most countries. Even in countries with a reporting system for infectious diseases, which are the major causes of ALD, there are few reliable data on the incidence of viral infection because reporting is not always mandatory and many cases are left unreported.

The Diagnosis Procedure Combination (DPC) database is a database containing discharge abstract and administrative claims of inpatients who are admitted to secondary or tertiary care hospitals in Japan [8–10], and represents approximately 40 % of inpatient admissions to such hospitals. The database contains a large number of samples, and can, thus, be used to investigate the incidence of ALD on an objective basis. The present study analyzed the incidence of admission related to ALD in Japan using the DPC database. In the database, clinical data to define the presence of ALF (i.e., prothrombin time, degree of encephalopathy, or length of illness) were not accessible. Therefore, we analyzed patients with ALD, who may include the entire cases of ALF, in a comprehensive manner. The aim of the present study was to collect detailed information on the clinical consequences for hospitalized ALD patients and estimate the public health burden of ALD in Japan.

Materials and methods

Data source

The DPC database contains the following information: hospital location; patient demographics; diagnosis, comorbidities at admission, and complications after admission recorded with Japanese text and International Classification of Diseases and Related Health Problems, Tenth Revision (ICD-10) codes; therapeutic procedures encoded by Japanese original codes; length of stay; discharge status, including in-hospital death; and total costs. A survey of the DPC hospitals is conducted by the DPC Study Group between 1 July and 31 December each year, and is funded by the Ministry of Health, Labour and Welfare, Japan. All 82 university teaching hospitals in Japan are obliged to adopt the DPC system, whereas adoption by community hospitals is voluntary. The survey started in 2003 with 82 teaching hospitals, and the numbers of participating hospitals and registered patients have since increased. The numbers of cases in the database were 2.99, 2.86, 2.57, and 3.19 million in 2007, 2008, 2009, and 2010, respectively, and represented approximately 40 % of all inpatient admissions to secondary and tertiary care hospitals in Japan.

The requirement for informed consent was waived in this study, because of the anonymous nature of the data. Study approval was obtained from the institutional review board of The University of Tokyo.

Samples

We obtained impatient data for 2007–2010. First, we identified patients with ICD-10 code-based diagnoses of hepatitis by any causes (ICD-10 codes, K70–K77), and those with viral, bacterial, or parasitic infections that may cause ALD through infectious diseases (A00–B99), from the 11.61 million inpatients included in the DPC database for 2007–2010. We then identified patients with Wilson's disease (E830), Budd–Chiari syndrome (I820), and acetaminophen overdose (T391), which are independent from the items of hepatitis (K70–K77) in the DPC database. Second, we manually checked the registered diagnoses in the Japanese texts for all of the screened cases to confirm the diagnosis of ALD. We excluded cases with a "suspected" diagnosis. We then excluded cases with diagnoses of chronic hepatitis (B170, B180–B189, K713–K715, and K721–K739) and liver cirrhosis (K702, K703, K717, K740–K742, K745, and K746) as well as cases with gastric and esophageal varices (I850, I859, and I864), which may imply the presence of chronic hepatitis. We also excluded cases with malignancy and those with a past history of liver transplantation.